

FMH606 Master's Thesis 2021
Process Technology

Investigation of the performance of a pilot-scale CO₂ desorption column using CFD simulations

Avishan Shakeri

Faculty of Technology, Natural sciences and Maritime Sciences
Campus Porsgrunn

Course: FMH606 Master's Thesis, 2021

Title: Investigation of the performance of a pilot-scale CO₂ desorption column using CFD simulations

Number of pages: 69

Keywords: CFD, OpenFOAM, Desorption column, Stripper, CO₂ desorption column, CO₂ Stripper, CFD desorption column, CFD Stripper, OpenFOAM desorption column, OpenFOAM Stripper

Student: Avishan Shakeri

Supervisor: Sumudu Karunaratne, Lars Erik Øi, Knut Vågsæther, Gamunu Samarakoon, Ismail Shah

External partner: Gassnova, Mongstad (Ismail Shah)

Summary:

Technology Center Mongstad (TCM) is the world's largest and most flexible test facility for amine based CO₂ absorption and desorption. This master thesis is based on an operational problem at TCM where excess liquid loading is experienced at water inlet (from the distributor) to the packing section of a CO₂ desorption column. This work is mainly focused on creating a CFD simulation of the stripper while having the geometry and problem of the TCM desorber column in mind for further improvements.

A literature search on CFD simulations on CO₂ stripper, absorber and packing has been carried out. A 2D laminar CFD simulation of a CO₂ capture stripper has been conducted using volume of fluid (VOF) method by OpenFOAM. The objective of this task is to perform a CFD simulation of a liquid flow distribution at the inlet of the packing area where the packing area is simulated as a porous zone.

The porous media is implemented in the middle of the desorber column where its performance is evaluated by observing the change in pressure in that zone. Illustrations showing the liquid phase distribution and relations to the change of pressure and velocity along y-axis have been simulated and evaluated. A case study on velocity and Darcy value has been conducted to see its result on liquid distribution on the packing area. The velocity ranges between 0.1 [m/s] to 2 [m/s] and the Darcy coefficient of Darcy-Forchheimer equation between 100 to $8.85 \cdot 10^{10}$ (The value evaluates permeability of the liquid to the porous zone). The results on this report do not point any solution for the problem but it gives a base case to work further to solve the problem.

In order to improve the current CFD simulation work, reactingMultiphaseEulerFoam solver can be a better choice for this case. Further creating the geometry of the packing in a CAD software and implementing that geometry into OpenFOAM can give more valid results than using a porous media.

Preface

This thesis was carried out as a part of the requirements for master's degree in Process Technology at University of South-Eastern Norway in Porsgrunn with cooperation with Technology Center Mongstad.

I would like to thank my supervisors, Dr. Lars Erik Øi, and Dr. Sumudu Karunaratne and my co-supervisor professor Knut Vågsæther and Gamunu Samarakoon for their great support and guidance throughout this work. I also thank the library of University of South-Eastern Norway for providing me with the necessary documents.

I would specially wish to thank my beloved parents, Soudabeh and Farshad, for their selfless support and love during my whole life and for giving me strength to reach for the stars and chase my dreams. My grandmother for her encouragement in many moments in the past months.

At the end, I express my appreciation to my boyfriend Julien Perdriau for motivating and helping me during my studies.

Porsgrunn, 19.May.2021

Avishan Shakeri

Contents

1	Introduction	10
1.1	Process description	10
1.2	Problem description	10
1.3	Objectives	11
1.4	Scope	11
2	Literature review	12
2.1	Computational fluid dynamics	15
2.1.1	<i>Pre-processor</i>	15
2.1.2	<i>Solver</i>	15
2.1.3	<i>Post-processor</i>	16
2.2	Conservation laws	16
2.2.1	<i>Mass conservation</i>	16
2.2.2	<i>Momentum conservation</i>	17
2.2.3	<i>Energy conservation</i>	17
2.3	Navier-Stokes equation	18
2.4	Finite volume method (discretization schemes)	19
2.5	Solver	21
2.6	Porous zone	21
2.7	Eulerian Multi-Phase and VOF Modeling	23
3	CFD MODELING	25
3.1	OpenFOAM CFD software	25
3.2	OpenFOAM file structure	25
3.2.1	<i>System</i>	25
3.2.2	<i>Constant</i>	30
3.2.3	<i>0</i>	31
3.3	Running the simulation	32
4	Results	33
4.1	Geometry and Mesh	33
4.2	Development of liquid phase fraction and velocity	35
4.3	Simulation comparison for case 2 to 4	41
4.4	Delta P over porosity	45
4.5	Velocity in the packing	47
5	Discussion	50
5.1	Discussion of uncertainties	50
5.2	Evaluation of alternative simulations	50
5.3	Discussion for further works	51
6	Conclusion	52
	References	53

Nomenclature

C_μ	Dimensionless constant
S_E	Source of Energy
S_{ij}	Rate of deformation
S_{Mx}	Source term for x-momentum
S_{My}	Source term for y-momentum
U_1	Volume average velocity of inlet
U_2	Volume average velocity of outlet
\vec{u}	Velocity vector $\begin{pmatrix} u \\ v \\ w \end{pmatrix}$
δ_{ij}	Kronecker Delta symbol equal to identity matrix $3 = \begin{pmatrix} 1 & 0 & 0 \\ 0 & 1 & 0 \\ 0 & 0 & 1 \end{pmatrix}$
μ	Viscosity [Pa.s]
μ_t	Eddy viscosity
τ_{ij}	The stress component acting in j-direction on a surface normal to i-direction
2D	Two dimensional
3D	Three dimensional
A	Surface area [m ²]
c	Specific heat [J/kg.k]
CCS	Carbon Capture and Storage
CFD	Computational Fluid Dynamics
CHP	Combined Heat and Power
CO ₂	Carbon dioxide
div	Divergence
E	Energy [J]
grad	Gradient
IEA	International Energy Agency
IPCC	Intergovernmental Panel on Climate Change

k	Material's conductivity in Fourier's law
L	Characteristic length
LES	Large eddy simulation
MEA	Monoethanolamine
p	Pressure (a normal stress)
PCC	Post Combustion Capture
PISO	Pressure-implicit split-operator
R	Ideal Gas Constant = 8.314 [J/k.mol]
RANS	Reynolds-Averaged Navier-Stokes
RAS	Reynolds-Averaged Simulation
Re	Reynolds number
SIMPLE	Semi-implicit method for pressure-linked equations
T	Temperature [k]
TCM	Technology Center Mongstad
u	Velocity in x-direction
U	Characteristic velocity in Reynolds equation
U	Mean Velocity Component
u'	Fluctuating velocity component in x-direction
v	Velocity in y-direction
v'	Fluctuating velocity component in y-direction
VOF	Volume of Fluid
Γ	Diffusive Coefficient [m^2/s]
ν	Kinematic viscosity [m^2/s]
ρ	Density [kg/m^3]
τ	Viscous stress/ Shear stress
ϕ	Flow variable

List of figures

Figure 1-1 CO ₂ capture process at Technology Center Mongstad (TCM) [1]	11
Figure 2-1 Geometry with porosity.....	22
Figure 3-1 OpenFOAM case directory of laminar case.....	26
Figure 3-2 Sketch of hexagonal blocks of the domain	27
Figure 3-3 Zoomed picture of the bottom left side of the hexagonal blocks sketch.....	28
Figure 4-1 2D geometry of stripper in cartesian coordinate	34
Figure 4-2 Wireframe view of geometry	34
Figure 4-3 Wireframe view of rescaled geometry	35
Figure 4-4 Velocity field for case 3 at time 0 (s).....	36
Figure 4-5 Velocity field for case 3 at time 0.5 (s).....	36
Figure 4-6 Velocity field for case 3 at time 1 (s).....	37
Figure 4-7 Velocity field for case 3 at time 7.5 (s)	37
Figure 4-8 Velocity field for case 3 at time 8.5 (s).....	38
Figure 4-9 Velocity field for case 3 at time 10 (s).....	38
Figure 4-10 Liquid phase fraction at time 0 (s)	39
Figure 4-11 Liquid phase fraction at time 0.5 (s)	39
Figure 4-12 Liquid phase fraction at time 1(s)	40
Figure 4-13 Liquid phase fraction at time 4.5 (s)	40
Figure 4-14 Liquid phase fraction at time 10 (s)	41
Figure 4-15 velocity profile of case 2 at time steps 0.5, 1 and 7.5 from left to right	42
Figure 4-16 Velocity profile of case 3 at time steps 0.5, 1, 7.5, 8.5, 10 from left to right	42
Figure 4-17 Velocity profile of case 4 at time steps 0.5, 1, 7.5, 8.5, 10 from left to right	43
Figure 4-18 Velocity profile of case 5 (U=0.1 m/s) at time steps 0.5, 1, 7.5, 10.....	43
Figure 4-19 Velocity profile of case 6 (U=0.5 m/s) at time steps 0.5, 1, 7.5, 10.....	44
Figure 4-20 Pressure difference in case 1 over y-axis.....	45
Figure 4-21 Pressure difference in case 2 over y-axis	45
Figure 4-22 Pressure difference in case 3 over y-axis.....	46
Figure 4-23 Pressure difference in case 4 over y-axis.....	46
Figure 4-24 Pressure difference in case 5 over y-axis.....	47
Figure 4-25 Pressure difference in case 6 over y-axis.....	47
Figure 4-26 Velocity distribution of case 1 along y-axis at time = 6 (s)	48
Figure 4-27 Velocity distribution of case 3 along y-axis at time = 6 (s)	48
Figure 4-28 Velocity distribution of case 4 along y-axis at time = 6 (s)	48
Figure 4-29 Velocity distribution of case 5 along y-axis at time = 6 (s)	48
Figure 4-30 Velocity distribution of case 6 along y-axis at time = 6 (s)	49
Figure 4-31 Velocity distribution of case 7 along y-axis at time = 6 (s)	49

List of tables

Table 2-1 Review of CFD simulation literatures on absorber, stripper and structured packing (part1/3).....	12
Table 2-2 Review of CFD simulation literatures on absorber, stripper and structured packing (part2/3).....	13
Table 2-3 Review of CFD simulation literatures on absorber, stripper and structured packing (part3/3).....	14
Table 2-4 Numerical discretization schemes	19
Table 2-5 Discretization schemes options for each term	20
Table 3-1 Discretization schemes used for each term of this simulation	30
Table 3-2 Boundary conditions for the laminar system.....	31
Table 4-1 Different velocity and Darcy coefficient values for case studies	33

1 Introduction

Computational fluid dynamics (CFD) is used for analyzing complex problems related to fluid flows in a system. Prediction of heat and mass transfer, studying the change in velocity, volume fraction, pressure and some other parameters in the system is possible with CFD simulation. In this introductory chapter process description, problem description and objective of this master thesis are accounted for.

1.1 Process description

Technology Center Mongstad is a post combustion capture (PCC) testing facility located in Mongstad, Norway. This facility uses MEA solvent to perform CO₂ capture. The process of amine based CO₂ capture at Technology Center Mongstad can be seen in Figure 1-1 [1]. The combined heat and power (CHP) stripper is the focus of this work. There are two strippers working independently in this process, one with diameter of 1.3 m and the other 2.2 m. Each stripper is designed to separate different CO₂ content. The purpose of the stripper is to recover MEA solvent and to remove CO₂ from the liquid phase. The stripper columns are divided into two separate packed beds with an inter-bed liquid distributor within the beds.

As it can be seen, low temperature rich solvent enters the stripper after passing through a cross current heat exchanger. The solvent inlet enters the top of the stripper column and flows downwards to the bottom of the desorption column. After desorption of CO₂ lean MEA solvent exists the bottom of the column. Then, it is cooled in the cross heat exchanger by low temperature rich amine and further with lean amine cooler to be used in the process again. Lighter components like CO₂ together with vapor water evaporate in the system due to the generated heat by the reboiler. The reboiler has a temperature between 110 to 125 °C. The rich loading contacts counter-current stripping vapor and absorbs energy for CO₂ desorption [2]. CO₂ product exits the top of the column and condensates to get collected at CO₂ stack [1].

1.2 Problem description

The motivation of this master thesis was originally based on an operation problem at Technology Center Mongstad. During the period of this work slight changes in the objective occurred due to lack of time and non-existence of base case. In this study, CFD analysis of a combined heat and power (CHP) stripper has been conducted. There is 8 meters of Flexipac 2X structured packing inside the desorption column [1]. The first task of this work is to create a base case CFD model of a CO₂ desorption column of industrial-scale pilot plant. The liquid phase distribution in the system, precisely when it reaches the packed area is the main focus of this work. The sizing of this column and other consideration and simplification is based on the TCM desorption column so that it can be used for further works to solve the operational problem.

1.3 Objectives

The main objective of this work is to simulate packed part of CO₂ stripper at TCM with OpenFOAM to visualize the liquid distribution when it flows in the packing. In order to achieve this, these steps were conducted:

1. Literature study on CFD modeling of desorbers and absorbers.
2. Geometry and mesh generation of CHP stripper with OpenFOAM.
3. Implementation of porous zone in the system.
4. CFD simulation of multiphase flow in laminar condition.
5. Analyzing the results for liquid distribution, change in velocity and pressure.

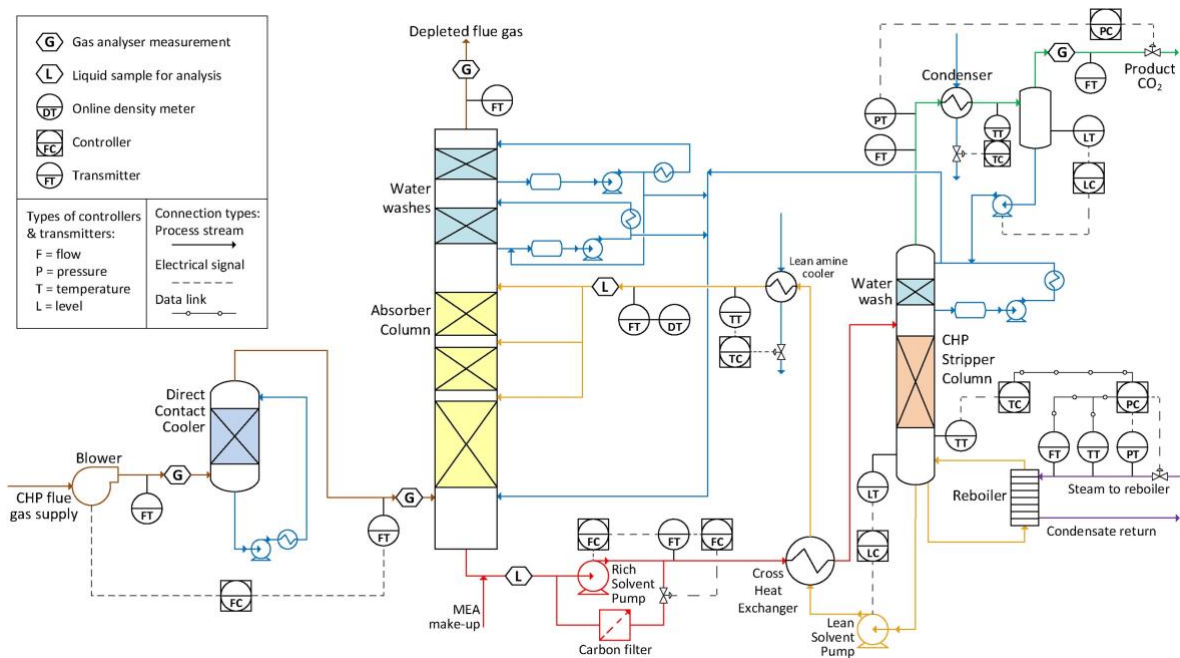


Figure 1-1 CO₂ capture process at Technology Center Mongstad (TCM) [1]

1.4 Scope

In the following part of this report, a literature study related to absorbers, desorbers and packing area CFD simulations is performed. Further, CFD theory and OpenFOAM simulation options for solving CFD equations are discussed before executing the simulation. Lastly, the simulation setting of this case is stated before publishing the results of the simulation work.

2 Literature review

According to Intergovernmental Panel on Climate Change (IPCC) the earth is facing a global warming of 1.5 °C between year 2030 to 2052 if it continues to increase with the current rate. It is vital to maintain the global temperature increase below this level [3]. Greenhouse gases like CO₂ have an intense impact on the global warming and delay in reduction of CO₂ emission can be very catastrophic [4]. Carbon capture and storage (CCS) technology has a potential to play a significant role in reduction of CO₂ emission. Currently, CO₂ emissions has the second largest emission in history by 1.5 billion tones in 2021 according to International Energy Agency (IEA). That is why the topic of carbon capture is of extreme importance. Due to the economic recovery of Covid crises there is a resurgence of using coal in the power sector which is not sustainable for climate. Coal power plants, oil-related emissions and CO₂ emissions from natural gas contribute mainly to emission of CO₂ [5].

An example of PCC process was illustrated in Figure 1-1 [1]. Despite the numerous studies of the CO₂ absorption column process, only a few were dedicated to study the CO₂ stripper. Since there are similarities in terms of modeling between the two systems, among all, some literatures on absorption column that were helpful for this work are listed in Table 2-1, Table 2-2 and Table 2-3.

Table 2-1 Review of CFD simulation literatures on absorber, stripper and structured packing (part1/3)

Reference	Work	Results	Model
Niegodajew et al. (2016) [6]	<ul style="list-style-type: none"> ▪ Numerical modeling of amine based absorber ▪ Chemical reaction and heat transfer considered ▪ Random packed bed ▪ Variation in lean loading (mol CO₂/mol MEA), solvent to flue gas ratio and CO₂ content 	<ul style="list-style-type: none"> ▪ Removal efficiency weakly dependent on CO₂ content if Amine solution loading is high ▪ CCS installation accuracy under changeable conditions 	<ul style="list-style-type: none"> ▪ Counter current gas-liquid ▪ Eulerian model ▪ 2D ▪ Laminar flow ▪ ANSYSYS ▪ FLUENT
Isoz (2017) [7]	<ul style="list-style-type: none"> ▪ CFD model of gas flow in distillation column through two structured packing: Mellapak 250.X and Mellapak 250.Y ▪ Study of gas mixing capability of the packing 	<ul style="list-style-type: none"> ▪ Construction of gas flow through structured packing ▪ Study the flow characteristics in Mellapak structured packing 	<ul style="list-style-type: none"> ▪ OpenFOAM ▪ 3D geometry (created with Blender)
Niegodajew et al. (2013) [8]	<ul style="list-style-type: none"> ▪ CFD model of amine based desorber ▪ Desorption reaction, multiphase heat transfer, evaporation/condensation phenomena considered 	<ul style="list-style-type: none"> ▪ Complex system of stripper was modeled ▪ Desorption efficiency are sensitive to key process parameters 	<ul style="list-style-type: none"> ▪ Eulerian gas-liquid ▪ Counter-current flow ▪ ANSYSYS ▪ FLUENT ▪ 2D

Table 2-2 Review of CFD simulation literatures on absorber, stripper and structured packing (part2/3)

Reference	Work	Results	Model
Gbadago et al. (2020) [9]	<ul style="list-style-type: none"> CFD model of MEA absorption process in different absorber configurations (single bed, double bed and 5 beds) AMT-SP 350Y structured packing Study of liquid hold-up, pressure drop and CO₂ removal efficiency 	<ul style="list-style-type: none"> Higher absorption rate in multi-bed columns Lower pressure drops in single bed and double bed absorber In low liquid loading, higher gas flow rates reduce the absorption efficiency Double packed beds are the most optimum Liquid hold-up is a key element in absorption efficiency Initial carbon loading of less than 30 % mol is the most efficient 	<ul style="list-style-type: none"> Eulerian multiphase model 3D k-ε model turbulence model OpenFOAM reactingTwoPhaseEulerFoam
Yang et al. (2018) [10]	<ul style="list-style-type: none"> Multiphase counter-current flow Visualization of liquid distribution, wettability and film thickness on structured packing 	<ul style="list-style-type: none"> Increase of dead zones at higher liquid Weber number (high liquid flow rates) Flooding happens at high Weber number Increase of Weber number together with inertial forces and surface tension leads to more uniform liquid distribution Liquid flow rate effects the wetted surface area and average film thickness Gas flow rate does not affect wetted area and liquid film thickness that much Higher gas flow rate causes large amount of liquid droplet generation 	<ul style="list-style-type: none"> 3D VOF Counter-current gas-liquid flow Large eddy simulation (LES)
Haroun et al. (2012) [11]	<ul style="list-style-type: none"> Mass transfer and liquid hold-up in structured packing Liquid hold-up and mass transfer as a function of liquid flow rate (according to Reynolds number and packing geometry) 	<ul style="list-style-type: none"> At low liquid flow rates we have uniform liquid film with low thickness Increase in liquid flow rate causes static hold-up (recirculation zone) forms in cavities and the liquid film thicken Increase of Reynolds number result in increase of static hold-up Mass transfer not affected by the static hold-up 	<ul style="list-style-type: none"> 2D VOF Co-current gas-liquid flow Laminar liquid film

Table 2-3 Review of CFD simulation literatures on absorber, stripper and structured packing (part3/3)

Reference	Work	Results	Model
Yu et al. (2018) [12]	<ul style="list-style-type: none"> ▪ Wave like structured packing ▪ Effect of surface texture on mass transfer, wetted area and liquid thickness 	<p>Comparison between WPA packing (rough surface) and Mellapak 125.X (smooth surface):</p> <ul style="list-style-type: none"> ▪ 2D VOF: Larger average film thickness compared to smooth surface mainly for low liquid loads ▪ 3D VOF: Similar flow paths, more wetted area in rough surface ▪ Higher liquid holdup on rough surface ▪ Inconsiderable pressure drop difference ▪ Better mass transfer on rough surface especially for low liquid loads 	<ul style="list-style-type: none"> ▪ ANSYSYS FLUENT ▪ 2D VOF & 3D VOF ▪ Counter-current gas-liquid ▪ RNG k-ε model
Pham et al. (2015) [13]	<ul style="list-style-type: none"> ▪ MEA absorber ▪ Mellapak 500.X is used as structured packing ▪ Packed area considered as porous zone ▪ Coarse, medium and fine mesh was performed ▪ Medium mesh used for further works ▪ Validity of porous media ▪ Includes porous resistance force, gas-liquid momentum exchange and liquid dispersion force in the momentum conservation ▪ Chemical reaction in liquid phase included 	<ul style="list-style-type: none"> ▪ Coarseness of the mesh effects the pressure drop and removal efficiency 	<ul style="list-style-type: none"> ▪ Eulerian gas-liquid ▪ 3D ▪ ANSYSYS FLUENT ▪ Effect of turbulence is ignored in porous zone
Raynal et al. (2008) [14]	<ul style="list-style-type: none"> ▪ CFD simulation of structured packing ▪ In 3D simulation: Mesh size and turbulence influence on pressure drop ▪ In 2D simulation: liquid hold-up determination 	<ul style="list-style-type: none"> ▪ Wet pressure drop can be predicted by combining dry pressure and liquid hold-up ▪ Dry pressure drop determined from 3D modeling ▪ Liquid hold-up determined from 2D two phase simulation 	<ul style="list-style-type: none"> ▪ 3D RNG turbulent model ▪ 2D VOF ▪ Co-current gas-liquid

In the present work, a 2D CFD simulation of CO₂ capture stripper, the second step of post combustion capture (PCC) with structured packing has been conducted with VOF approach for a pilot scale facility. The packing structure has been simulated as a porous zone. The focus of this work is on distribution of the liquid flow on packing area of a single bed column below a distributor. This study covers laminar flow of rich loading into the desorber. CFD software OpenFOAM (finite volume based solver) is used for this simulation and ParaView is a visualization tool for post-processing.

2.1 Computational fluid dynamics

Most of the theoretical information about CFD in this chapter is taken from the book “*An Introduction To Computational Fluid Dynamics Finite Volume Method*” [15].

Commercial CFD packages such as OpenFOAM have interfaces where user can input problem parameters to get the result. The codes contain three elements:

- Pre-processor
- Solver
- Post-processor

2.1.1 Pre-processor

In pre-processor stage the computational domain of the geometry is created. Then this domain is being meshed where each cell is divided into smaller and finer sub-domain. These cells are so called control volumes of the system where CFD calculation is happening. The finer the mesh the more accurate the solution. A very fine mesh demands an expensive computational cost. For this reason, it is important to find the optimal mesh in the system. Have finer mesh in the area facing lots of changes and more coarse mesh where the system is more steady. Furthermore, the fluid properties such as density and viscosity is chosen in this stage in addition to boundary and initial conditions of the system for velocity, pressure, temperature, volume fraction, etc.

2.1.2 Solver

There are several well-known numerical methods and the one OpenFOAM uses to solve CFD problems is the finite volume method. The finite volume method integrates the governing equations over all control volumes in the domain. It then converts partial differential equations to algebraic equations which is called discretization. All algebraic equations are solved simultaneously by iterative method. Conservation of flow variables such as velocity is expressed by finite volume method within each cell.

Imagine a flow variable ϕ in the statement below is applicable in each cell of the domain. The CFD codes contain discretization schemes to solve each term of the statement iteratively.

Rate of change of ϕ in the control volume	=	Net rate of increase in ϕ due to convection in the control volume	+	Net rate of increase in ϕ due to diffusion in the control volume	+	Net rate of creation of ϕ in the control volume
--	---	--	---	---	---	--

2.1.3 Post-processor

A computer application ParaView is used to visualize the work done in the pre-processing. This visualization can be the geometry and mesh as well as how the simulation runs, figures and vectors to see the result of the simulation.

Prior to adjusting the setting and running the simulation, the physical and chemical phenomena of the problem should be taken into consideration. To have a good model we are required to make the right choices. There are always assumptions to simplify the task and reduce the complexity. Some of these considerations for this case is listed below:

- 2D model
- Laminar flow
- Neglected heat transfer
- Neglected chemical desorption reaction
- Incompressible fluid (constant density)
- Isotropic fluid (uniform properties in all directions)
- Newtonian fluid (viscous stress is linearly correlated to deformation rate)

2.2 Conservation laws

Base on conservation laws of physics three criteria should be considered:

- Mass conservation
- Momentum conservation (Newton's second law)
- Energy conservation (First law of thermodynamics)

It should be noted that all the equations in this chapter are written for a x-y cartesian system.

2.2.1 Mass conservation

Mass conservation by definition implies that the rate of increase of mass in fluid element is equal to the net rate of flow of mass into fluid element. Writing the mass conservation (Continuity equation) in cartesian system for an incompressible fluid results in:

$$\frac{\partial \rho}{\partial t} + \text{div}(\rho \vec{u}) = 0 \quad (2.1)$$

The second term is a convective term defining the net flow of mass. In case of incompressible fluid ρ is constant and the continuity equation will be:

$$\text{div } \vec{u} = 0$$

Considering the fact that our case is a 2D case:

$$\frac{\partial u}{\partial x} + \frac{\partial v}{\partial y} = 0 \quad (2.2)$$

2.2.2 Momentum conservation

By definition from the Newton's second law rate of change on fluid particle equals to the sum of forces on fluid particle. There are pressure forces and viscous forces applying on fluid particles. The pressure force is denoted by p and the viscous force by τ . The momentum conservation equations for 2D case are as shown below:

x-momentum:

$$\rho \frac{Du}{Dt} = \frac{\partial(-p + \tau_{xx})}{\partial x} + \frac{\partial\tau_{yx}}{\partial y} + S_{Mx} \quad (2.3)$$

y-momentum:

$$\rho \frac{Dv}{Dt} = \frac{\partial\tau_{xy}}{\partial x} + \frac{\partial(-p + \tau_{yy})}{\partial y} + S_{My} \quad (2.4)$$

2.2.3 Energy conservation

The conservation of energy is defined by the first law of thermodynamics as:

Rate of increase of energy of fluid particle is sum of net rate of heat added to the fluid particle and net rate of work done on the fluid particle.

$$\rho c \frac{DT}{Dt} = \tau_{xx} \frac{\partial u}{\partial x} + \tau_{yx} \frac{\partial u}{\partial y} + \tau_{xy} \frac{\partial v}{\partial x} + \tau_{yy} \frac{\partial v}{\partial y} + \text{div}(k \text{ grad } T) + S_E \quad (2.5)$$

It can also be written in term of internal energy E :

$$\rho c \frac{DE}{Dt} = \frac{\partial u \tau_{xx}}{\partial x} + \frac{\partial u \tau_{yx}}{\partial y} + \frac{\partial v \tau_{xy}}{\partial x} + \frac{\partial v \tau_{yy}}{\partial y} + \text{div}(k \text{ grad } T) - \text{div}(\rho u) + S_E \quad (2.6)$$

The fluid motion of a 2D system is described by equation (2.3) to (2.6) one mass conservation, two momentum conservations and one energy conservation equation. Since the fluid is

assumed to be incompressible, the unknowns in equations above can be solved by solving the momentum and continuity equations. In addition, in case of heat transfer in the system the energy equation is solved.

2.3 Navier-Stokes equation

Navier-Stokes equations are set of partial differential equations that describe the flow of incompressible fluid. These sets of equation describe how pressure, velocity, temperature and density of a moving fluid are related. They also include the effect of viscosity on the flow. The Navier-Stokes equation for 2D case include a time dependent continuity equation, two time dependent momentum conservation equations and a time dependent energy conservation equation. Navier-Stokes system is a coupled system of the four equations (2.3, 2.4, 2.5, 2.6) where all four equations should be solved simultaneously. The unknowns in this system are:

1. Pressure (p)
2. Density (ρ)
3. Temperature (T)
4. Velocity vector in x direction (u)
5. Velocity vector in y direction (v)

As it is described above, we have 4 equations and 5 unknown parameters. In order to be able to solve this set of equations we need one more equation and that is the equation of state (EOS) for the gas.

$$p = \rho RT \quad (2.7)$$

Moreover, we need the value of the stress tensors τ (viscous forces). Since the diffusion term is responsible for turbulence in the system these parameters will be approximated by turbulence model [16].

If we look at equation 2.3 to 2.6, we can see that there are things in common between these equations. Transport equation (equation 2.9) is a more common form of equation for parameter ϕ . Where if $\phi = 1$ the mass balance is produced, $\phi = u$ produces x-momentum, $\phi = v$ is y-momentum and $\phi = T$ is internal energy balance.

$$\frac{\partial(\rho\phi)}{\partial t} + \text{div}(\rho\phi u) = \text{div}(\Gamma \text{grad } \phi) + S_\phi \quad (2.8)$$

The first term in the left hand side of the equation is the transient term, the second term is convective term. The convective term is due to the movement of the fluid. The first term in the right hand side is the diffusion term and it is related to the viscosity of the gas. This term is responsible for turbulence and boundary layers in the system and the last term is the source term.

2.4 Finite volume method (discretization schemes)

To solve any set of equation in CFD software OpenFOAM we have to discretize each term of the equation. For example, explanation on each term of transport equation was given in subchapter 2.3. In

Table 2-4 a summary of each keyword and what they refer to is mentioned.

Table 2-4 Numerical discretization schemes

Term	Keyword	Discretizes the ... [17]
Time scheme	ddtSchemes	first order time derivative $\frac{\partial}{\partial t}$
Time scheme	d2dt2Schemes	Second order time derivative $\frac{\partial^2}{\partial t^2}$
Gradient scheme	gradSchemes	gradient ∇
Divergence scheme	divSchemes	divergence $\nabla \cdot$.
Laplacian scheme	laplacianSchemes	laplacian ∇^2
Interpolation scheme	interpolationSchemes	cell to face interpolations of values
Surface normal gradient scheme	snGradSchemes	component of gradient normal to a cell face
Other	wallDist	Distance to wall calculation, where required

OpenFOAM includes variation of discretization schemes but only quite few schemes are used for real life engineering problems. One way to choose which scheme to use for each term is to use the same schemes as in similar tutorials from OpenFOAM.

While choosing the right scheme we should have these three properties in mind:

- Conservativeness
- Boundedness
- Transportiveness

Conservativeness indicates that the values at the interface of each cell are the same. Boundedness assures that in case with no source in the cell, the value of φ is between its neighbors. At last, Transportiveness describes the influence of upstream and downstream nodes (node is at the centroid of each cell).

There are several discretization schemes for each term that can be chosen related to the criteria of the case we want. Information about finite volume schemes of each term can be found in [18] in more detail. In Table 2-5 a brief list of available discretization schemes for each term with their specifications can be found.

Table 2-5 Discretization schemes options for each term

Term		Discretization scheme	Specification
Time scheme (first order)		steadyState	$\frac{\partial}{\partial t} = 0$
		Euler	Transient, first order, bounded
		Backward	Transient, second order implicit, potentially unbounded
		CrankNicolson	Transient, second order implicit, bounded
		localEuler	Pseudo transient, first order implicit
Time scheme (second order)		Euler	-
Gradient schemes		Gauss linear	Primarily used
		cellLimited Gauss linear 1	Poor mesh, discretization of specific gradient terms are set aside (U, k or epsilon), bounded
		leastSquares	Second order
		Gauss cubic	Third order, appears in dnsFoam
Divergence schemes	Advection term	Gauss linear	Second order, unbounded
		Gauss linearUpwind grad(U)	Second order, unbounded (less than linear), requires discretization of velocity gradient
		Gauss LUST grad(U)	75% linear 25% linearUpwind, requires discretization of velocity gradient
		Gauss limitedLinear	Linear scheme that limits toward upwind in fast changing gradient regions
		Gauss upwind	First order, bounded, too inaccurate
		Gauss cubic	Rarely used
		Gauss vanLeerV	Rarely used, used for advection of scalar fields, less strong limiting than limiterLinear
	Diffusive term	Gauss linear	-
Surface normal gradient schemes		corrected	Second order, $\psi = 1$,
		Limited corrected 0.33	Second order, $\psi = 0.333$, greater stability, recommended for maximum non-orthogonality above 70°
		Limited corrected 0.5	Second order, $\psi = 0.5$, greater accuracy, recommended for maximum non-orthogonality above 70°
		orthogonal	Second order, Regular mesh in Cartesian coordinate, recommended for low non-orthogonal mesh
		uncorrected	First order, $\psi = 0$, recommended for low non-orthogonal mesh
Laplacian schemes		Gauss Linear <snGradSchemes>	-
Interpolation schemes		linear	Used in almost every case
		cubic	Used in cases such as: DNS on a regular mesh or stress analysis

2.5 Solver

To solve the momentum conservation equations in the Navier-Stokes equation set, we need an initial guessed value for pressure. With this pressure we achieve the value for the velocity but then this calculated velocity has to satisfy the mass conservation equation as well. This is what is called pressure-velocity coupling problem. In CFD software there are pressure-velocity coupling algorithms that solve these equations iteratively and simultaneously. Such numerical algorithms are: SIMPLE, PISO and PIMPLE. The SIMPLE algorithm is used for steady-state problems while the two other are used in transient cases.

2.6 Porous zone

The Porous media simulation is a valid choice for a packing since the mesh of the packing in a system can be very fine. Under circumstances like this the created mesh will be extremely fine and not practical because it drives the cell count too high. As a result, we consider using a porous zone instead of meshing the actual geometry [19]. Porous zone is the most important region of the simulation performance since it provides effective contact area between gas and liquid; hence it improves the mass transfer [10]. Packing types are random or structured which both provide the effective surface area but structured packing have an advantage of lesser pressure drop in the system.

Explanation on how the porous zone is formulated in CFD equations are explained in the following. Figure 2-1 illustrates a geometry with a porous zone where:

$$A_1 = A_2 \quad (2.9)$$

$$\rho U_1 A_1 = \rho U_2 A_2 \quad (2.10)$$

$$U_1 = U_2 \quad (2.11)$$

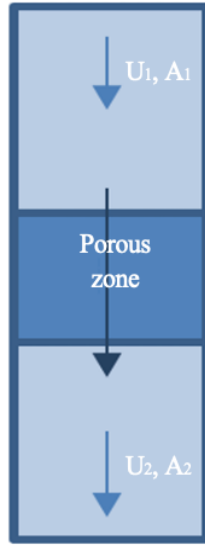


Figure 2-1 Geometry with porosity

Porous zone as an obstruction does not remove kinetic energy from the flow. However, it does still remove energy from the flow as a pressure drop. The pressure drop across the porous zone can be given as equation (2.12).

$$\Delta p = C_1 U + C_2 U^2 + C_3 U^3 + \dots \quad (2.12)$$

It is more common to use the first and the second term such as equation (2.13) where the second term is written as a dynamic head.

$$\Delta p = C_1 U + C_2 \frac{1}{2} \rho U^2 \quad (2.13)$$

What can be seen is that the faster the fluid flows through the obstruction the greater the pressure drop will be. It should be noted that the velocity used to calculate the pressure drop is volume averaged velocity U and not a superficial velocity U_s . The superficial velocity is the velocity between the gaps of the porous structure which is increased locally because the area has been reduced.

In order to model the porous media in CFD an additional source term (S) is added to the Navier-Stokes equations.

$$\begin{aligned} \frac{\partial(\rho \mathbf{U})}{\partial t} + \nabla \cdot (\rho \mathbf{U} \mathbf{U}) \\ = -\nabla p + \nabla \cdot \left(\mu \left((\nabla \mathbf{U}) + (\nabla \mathbf{U})^T \right) \right) - \frac{2}{3} \mu (\nabla \cdot \mathbf{U}) \mathbf{I} + \rho \mathbf{g} + S \end{aligned} \quad (2.14)$$

Indeed, the pressure drop is not added to the Navier-Stokes equation. The source term is zero in all the cells except from the cells of the porous zone. The unit of the source term is [Force/Volume] and it will be multiplied by the volume of cell when it is solved. Force has three components in the cartesian system x, y and z. In equation (2.15) to (2.18) the x direction is shown only and it will be the same sets of equations for the other directions as well.

$$\Delta p_x = C_1 U_x + C_2 \frac{1}{2} \rho |\mathbf{U}| U_x \quad (2.15)$$

$$F_x = -\Delta P_x A = -\left(C_1 U_x + C_2 \frac{1}{2} \rho |\mathbf{U}| U_x\right) A \quad (2.16)$$

$$S_x = \frac{F}{v} = -\left(C_1 U_x + C_2 \frac{1}{2} \rho |\mathbf{U}| U_x\right) \frac{1}{t} \quad (2.17)$$

$$S_x = \frac{F}{v} = -\left(\frac{C_1}{t} U_x + \frac{C_2}{t} \frac{1}{2} \rho |\mathbf{U}| U_x\right) \quad (2.15)$$

A is frontal area of cell and v is the volume of the cell. Unit of C1 is [kg/m³] and C2 [1/m]. The negative sign in equation (2.16) is because we are interested in the force on the liquid flow and not the solid. Term t in equation (2.17) is the thickness of porous zone in the direction of the flow.

The source term is combined of two terms, a viscous loss and inertial loss term which creates the pressure drop. Darcy-Forchheimer equation (2.19) describes the source term as a combination of these two terms.

$$S_x = -\left(\mu D + \frac{1}{2} \rho |\mathbf{U}| F\right) U_x \quad (2.19)$$

The idea behind this equation is that permeability (viscous drag through porosity) and form drag coefficient are connected. Form drag coefficient remarks that the internal geometry of porous medium causes flow blockage in system and this results in the pressure drop. This is the reason for different permeability of the flow in the system. A flow in Darcy regime permeated differently through porous zone than a flow in Forchheimer regime [20].

2.7 Eulerian Multi-Phase and VOF Modeling

Eulerian multi-phase modeling approach can account for both dispersed-continuous and continuous-continuous phase interactions. The dispersed phase can be solid particles, liquid droplets or gas bubbles. Dispersed phases are typically very small in order of micrometer or millimeter and are dissolved in the continuous fluid. The dispersed-continuous phase interaction is the interaction between these small particles or droplets and the continuous phase. On the other hand, the continuous-continuous phase interaction happens when two phases form a discrete interface. An example can be the interface between oil and water. In this sort of phase

interaction, the phases are immiscible in each other and there is a sharp interface between phases. The case in this master thesis is a dispersed-continuous phase interaction. The dispersed phase is CO₂ gas and the continuous phase is MEA. Eulerian model solves continuity and mass conservation equation for each phase and for this reason the Eulerian multiphase model is quite expensive.

Full Eulerian model can account for dispersed-continuous and continuous-continuous phase interaction. The simplified versions of the full Eulerian model are Mixture Models and Volume-of-fluid (VOF) model. The mixture model is used specifically for dispersed-continuous phase interaction and the VOF for continuous-continuous phase interaction. Mixture models and VOF models solve a single continuity equation. These models solve a single continuity equation and are less expensive than Eulerian model.

3 CFD MODELING

Computational fluid dynamics (CFD) modeling is one of the most common and popular numerical modeling methods based on the principle of the fluid mechanics. It can help with a troubleshooting process and helping with a solution when a system does not function as anticipated. CFD models and algorithms attempt to simulate the interaction of gases and liquids where the surfaces are defined as boundary conditions. These models are based on the Navier-Stokes equations that are solved iteratively for either transient or steady state condition. OpenFOAM is an open source interface where the CFD simulations can be modeled and analysed. [21]

In this report the listed tools below have been used:

- OpenFOAM version 8
- PIMPLE algorithm
- interFoam solver
- Laminar condition

3.1 OpenFOAM CFD software

OpenFOAM is an application widely used in engineering because it is free and open source. It is being used both in commercial and academical contents. OpenFOAM has the ability to simulate complex fluid flows including so many factors such as turbulence and heat and mass transfer [22].

3.2 OpenFOAM file structure

The base case is similar to the existing tankFoamcase tutorial supplied Jose Lorenzo [23]. There are modifications done on the tutorial case which are explained in this chapter other than these changes the other files are kept as it is. The case directory of the current laminar simulation is shown in Figure 3-1.

3.2.1 System

The system directory consists of six dictionaries. The necessary explanations regarding each file are written in the following subchapters.

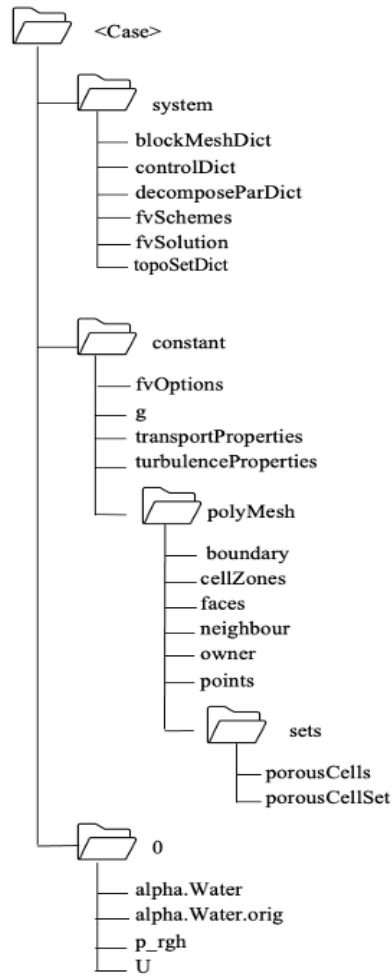


Figure 3-1 OpenFOAM case directory of laminar case

3.2.1.1 blockMeshDict

Information regarding the geometry, mesh generation and geometrical boundaries of the system is found in the blockMeshDict dictionary. The geometry of this case is made of 13 hexahedrons each defined by 8 vertices. A total of 96 vertices are defined (considering that the first vertex is labeled as 0). A sketch illustrating the blocks creating the geometry is shown in Figure 3-2. What is not very clear (due to the small size of the width of the block) is one block on the left and another on the right which is shown more clearly in Figure 3-3.

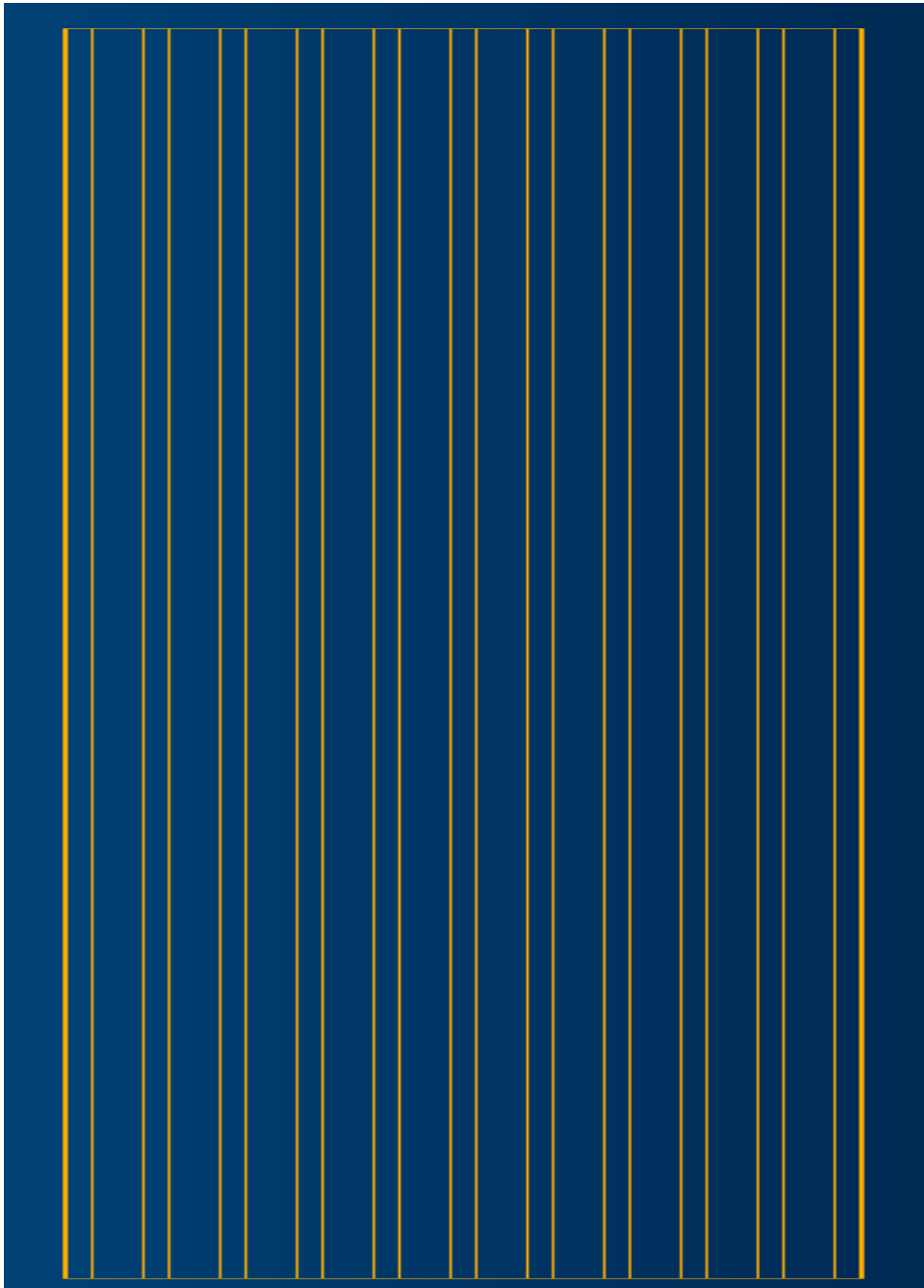


Figure 3-2 Sketch of hexagonal blocks of the domain

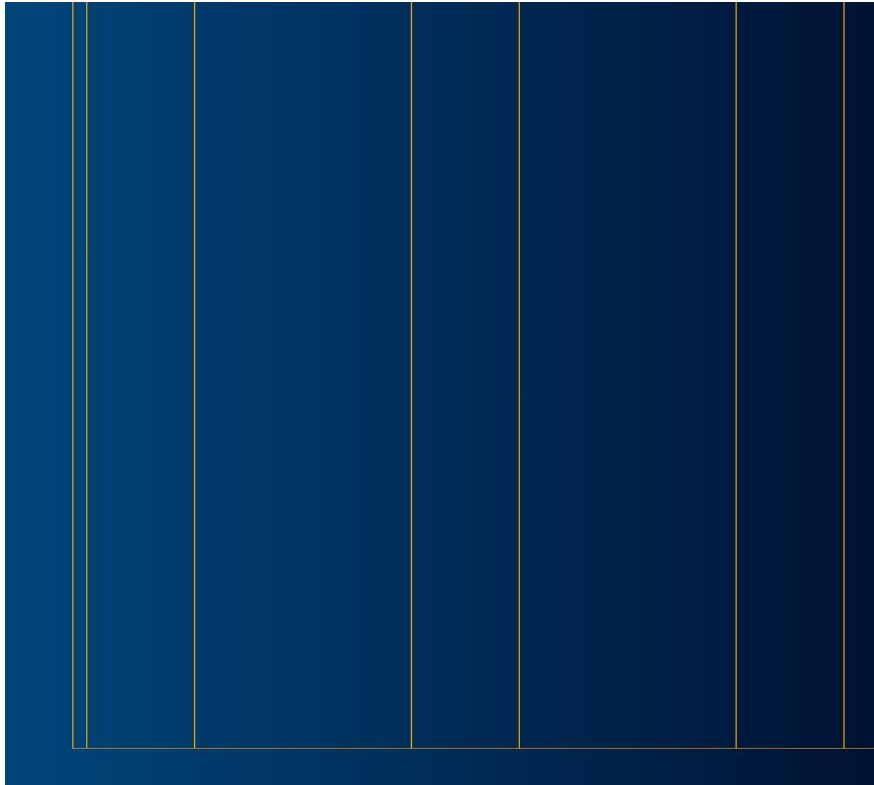


Figure 3-3 Zoomed picture of the bottom left side of the hexagonal blocks sketch

This dictionary starts with `convertToMeters` and since the dimensions in this dictionary are in meter the coefficient 1 is used. OpenFOAM works with 3D mesh by default but for simplification in this case a 2D geometry is created. The mesh is defined by number of cells in each direction of the block. There is only one cell along z -direction indicating that the simulation is 2D in x - y plain. `simpleGrading` shows that the cells have uniform expansion in all directions.

A choice of mesh size significantly affects the accuracy and numerical stability of CFD simulations. A fine mesh was tested for this case but due to a very demanding computational cost I have decided to follow the simulation with a medium mesh which is finer at the liquid inlet.

In addition, geometrical boundaries are defined in “boundary” subdirectory. The information about the boundary patch types is explained in Table 3-2 in section 3.2.3. The patch type “`symmetryPlane`” was chosen for the side walls to make the liquid continuously flow down “sandwich-like” according to [10] but since it did not give the expected flow behavior it is kept as a “wall”. The type “`patch`” is chosen for inlet and outlet and top side of the column since it does not contain any geometric or topological information [22].

The `blockMeshDict` setting file can be find in Appendix A.

3.2.1.2 topoSetDict

The topoSetDict file is used to define the porous zone in the column. Six meters of packing inside the column is simulated as a porous zone. It is very demanding to create the packing geometry and almost impossible with OpenFOAM. To be able to create the whole geometry with OpenFOAM and avoid using other applications it has been decided to consider the packing as a porous media.

It is important to notice that the unit used for coordinates of porousCellSet box is in meters regardless of the unit used defining the blockMeshDict file for vertices. The porous cells box is addressed by two coordinates, the bottom left front coordinate and the top right back coordinate of the box. Then, all the cells within these two points are considered as the porous media. The porous zone consists of 4950 cells (out of a total of 13200 cells).

In this thesis we are more interested in the behavior of the liquid after entering the packed section of the column. Therefore, we are simulating the column partly as a one packed bed column below the distributor.

In this file the geometrical region where the porosity source should be applied is defined. To involve the porosity in CFD calculations we must define another file named fvOptions in constant or system directory which is explained in section 3.2.2.4 .

The topoSetDict setting file can be find in Appendix B.

3.2.1.3 controlDict

All the settings about start time, end time and time interval are located in this folder. This case was simulated for 24 seconds but shorter time period could have given the results we are looking for so it then reduced to 10 seconds for all cases except from case 5. The reason for this was to see if the liquid distribution in the system will change in time for lower velocities or not.

The solver used for the simulation is interFoam a solver for two incompressible, isothermal immiscible fluids using VOF phase fraction interface capturing. This means that the properties for one phase (gas phase in this case) are constant in regions filled with liquid except at the interphase.

The controlDict setting file can be find in Appendix C.

3.2.1.4 fvschemes

All the discretization schemes are set in this dictionary. The options of choosing schemes are discussed in section 2.4 . The set ups of this dictionary do not differ from the base case.

It should be noted that the transient simulation is important to observe the growth of liquid film and development of gas-liquid interactions [10].

Table 3-1 Discretization schemes used for each term of this simulation

Keyword	Scheme
ddtSchemes	Euler
gradSchemes	Gauss linear
divSchemes	Gauss linearUpwind grad(U)
laplacianSchemes	Gauss linear corrected
interpolationSchemes	Linear
snGradSchemes	corrected

The fvSchemes file setting can be find in Appendix <D>

3.2.1.5 fvSolution

fvSolution directory has different subdirectories with information on solvers, tolerances and algorithms. First sub directory is about the solvers and for each discretized equation it specifies a linear solver that is used [24].

Some input parameters have to be implemented for each solver. For example, momentumPredictor control switch should be off for multiphase flows and flows with low Reynolds. nOuterCorrectors = 1 indicates that the system is solved once. nCorrectors is number of times that pressure equation and momentum is solved in each step (used only by PISO and PIMPLE). nNonOrthogonalCorrectors = 0 or 1 updates the explicit non-orthogonal correction term described in Table 2-5.

The fvSolution file setting can be find in Appendix <E>

3.2.2 Constant

This folder holds information regarding all properties of fluids as well as information about the gravitational acceleration. Subfolder polyMesh includes full description of the case mesh.

3.2.2.1 transportProperties

phaseProperties is a dictionary containing the information about the properties of two phases. There have been several experimental studies for MEA density value listed here: [25]. I have chosen an approximate value of 1006 kg/m³ from the work of Yang et al. [26].

The values for density and kinematic viscosity of CO₂ and MEA are set in this dictionary which can be seen in Appendix <F>

3.2.2.2 g

In this dictionary the value of gravitational acceleration and its direction is set. The value is 9.81 in negative y-axis direction.

3.2.2.3 turbulenceProperties

This is simulated for a laminar case.

3.2.2.4 fvOptions

The files regarding the porous media simulation are taken from a tutorial by Peyman Havaej and with a help from a two tutorials and ANYSYS FLUENT website [27] [28] [29].

This file is where we define the extra source term in Navier-Stokes equations for calculation of the porous zone. The “d” and “F” value are Darcy-Forchheimer D and F values in equation (2.19). The simulations in this work are assumed to be linear velocity-pressure drop relation therefore, the F value is set to 0 and we only consider Darcy contribution (linear resistance coefficient). Different tested Darcy values in this case are: 100, 200, 500e6 and 8.85e10.

fvOptions dictionary setting can be find in Appendix <G>

3.2.3 0

The 0 folder in OpenFOAM is the time directory. It is a folder where initial and boundary condition of different fields such as velocity, pressure, temperature, etc. is defined. In addition, after running the case the results of the field for each interval is written inside the file by OpenFOAM [30]. It is important to note that in OpenFOAM even in case of running a steady state simulation, the initial value of the fields should be given. The name of this folder is 0 referring to the start time of the simulation $t=0s$ which is specified in controlDict directory. A value should be assigned for all the patches that has been named in the blockMeshDict dictionary. Table 3-2 shows the information for each boundary field.

Table 3-2 Boundary conditions for the laminar system

Boundary name	type	Boundary field		
		U	p_rgh	alpha
inlet	patch	fixedValue	fixedFluxPressure	inletOutlet
outlet	patch	pressureInletOutletvelocity	totalPressure	zeroGradient
top	patch	noSlip	zeroGradient	zeroGradient
leftWall	wall	noSlip	zeroGradient	zeroGradient
rightWall	wall	noSlip	zeroGradient	zeroGradient

3.2.3.1 alpha

As mentioned before in this case we have two phases. Liquid MEA solvent and CO₂ gas phase after desorption. In this simulation we assume that the whole domain is filled with air at t=0 and the liquid phase fraction is 1 at the liquid inlet.

3.2.3.2 p_rgh

This file refers to the hydrostatic pressure and it is shown in the (3.7). Hydrostatic pressure is the pressure exerted by a fluid on an immersed body. Since in our case there is no immersed body the value set for this boundary condition is zero.

$$p_{rgh} = p - \rho gh \quad (3.1)$$

p is total pressure.

Simulation setting of alpha, p_rgh and U can be found in Appendix <H> <I> <J> respectively.

3.2.3.3 U

Different inlet velocity values have been tested in this work ranging from 0.1 m/s to 2 m/s.

3.3 Running the simulation

The following commands should be executed in the terminal window of the case directory:

1. blockMesh : to mesh the geometry
2. checkMesh: to check validity of the mesh
3. topoSet: to create the porous zone
4. interFoam: to run the solver
5. paraFoam: to visualize the solution in ParaView

4 Results

ParaView tool is used to visualize the transient solution of this simulation. This chapter is going to show the results of CFD simulations of a laminar case. The parameters that are changing in the simulation cases are the velocity of the liquid inlet and the Darcy coefficient from Darcy-Forchheimer equation (2.19). The results are reported as listed below:

- Geometry creation
- Mesh generation
- Development of one simulation case over different time steps
- Comparison of simulation view of different cases with variant Darcy values
- Comparison of simulation view of different cases with variant velocities
- Figure of the pressure drop in all simulated cases
- Comparison of pressure drops in cases with different velocity
- Comparison of pressure drop in Darcy value different cases
- Velocity development along the length of the column (y-axis)

The cases studied in this chapter are as below:

Table 4-1 Different velocity and Darcy coefficient values for case studies

Case	1	2	3	4	5	6	7
Velocity [m/s]	1	1	1	1	0.1	0.5	2
Darcy value [-]	100	200	$5 \cdot 10^8$	$8.85 \cdot 10^{10}$	$5 \cdot 10^8$	$5 \cdot 10^8$	$5 \cdot 10^8$

4.1 Geometry and Mesh

The geometry is made of 27142 points, 13200 cells and 53170 faces. 4950 cells are creating the porous zone of this system. Below (Figure 4-1) the geometry of the single bed stripper below the distributor is shown plus the meshing of the system (**Error! Reference source not found.** and Figure 4-3) which is more fine in hexagonal including the inlet patch. The fine mesh has been created for this case but since it required a high computational cost (around 12 hours per simulation) the work is performed mainly on the medium mesh. The height of the column is 8.05 meter and the diameter is 1.25m. The packing area is right below the distributor in the main geometry but here, in order to be able to visualize the fluid flow in the system clearly, I have changed the porous region location to the center of the column from y=3 to y=6.

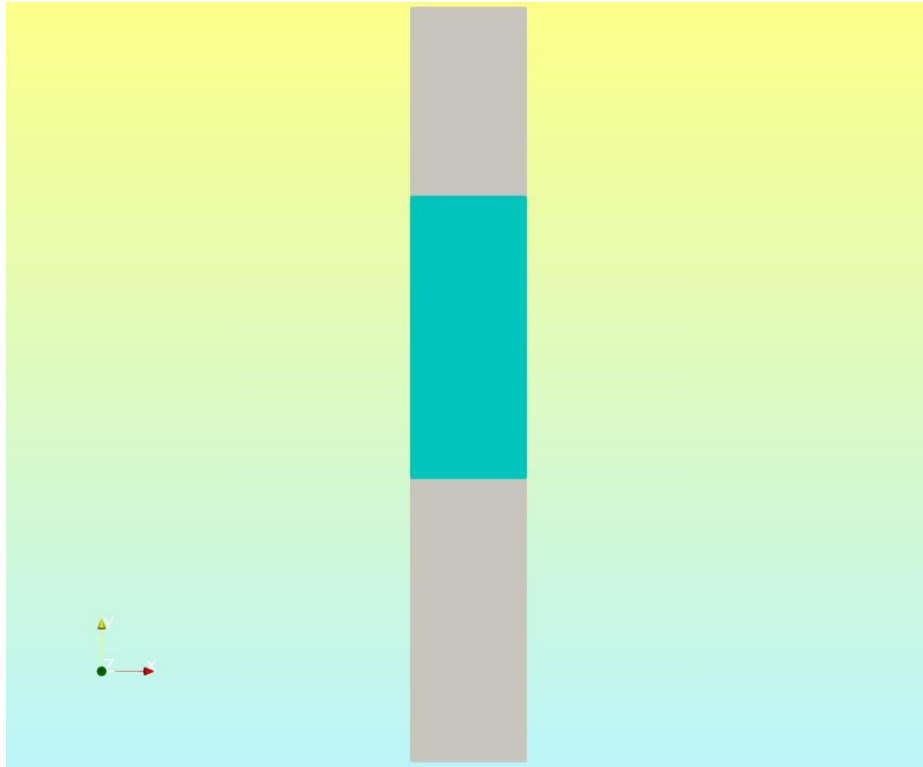


Figure 4-1 2D geometry of stripper in cartesian coordinate

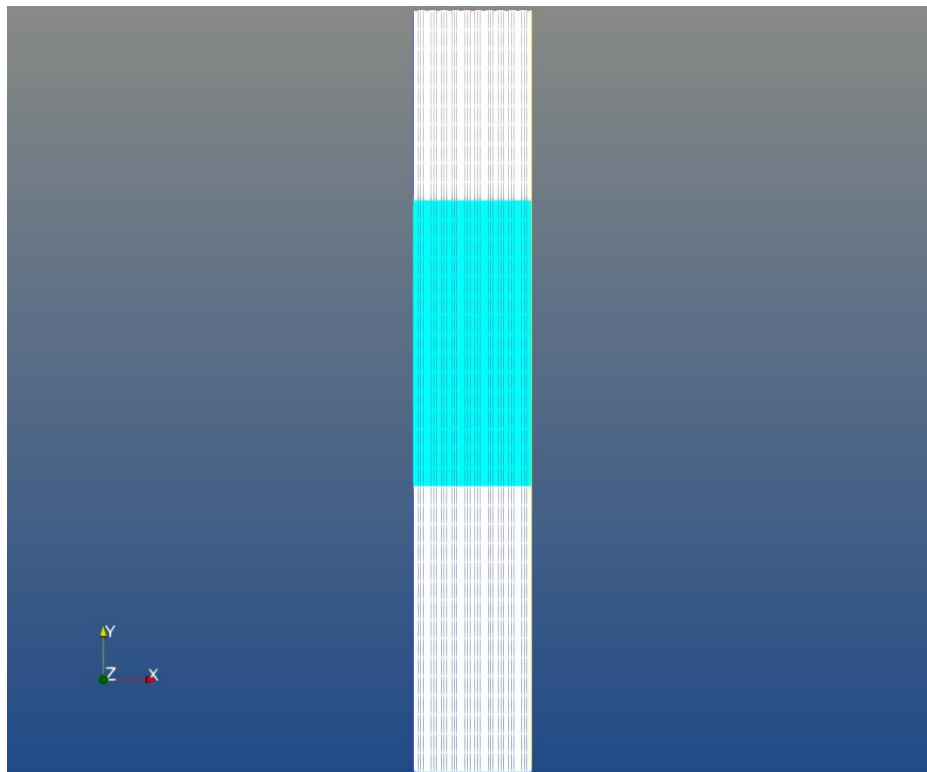


Figure 4-2 Wireframe view of geometry

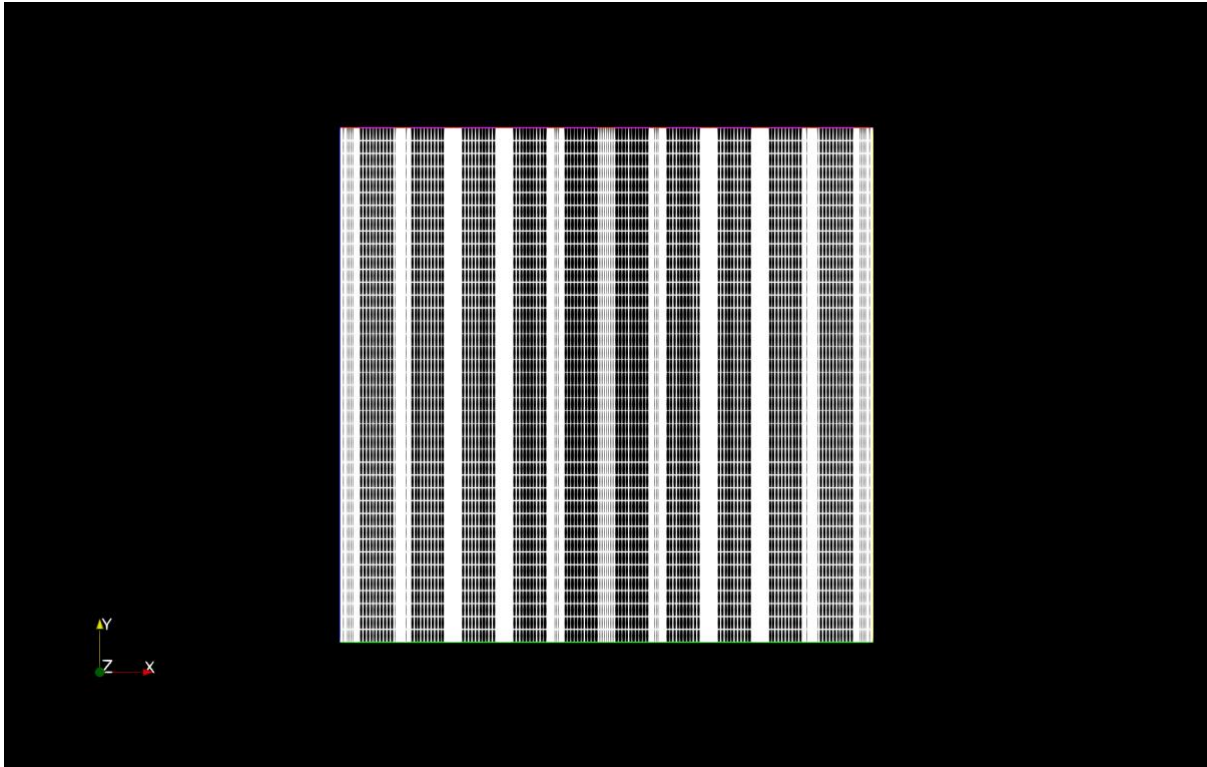


Figure 4-3 Wireframe view of rescaled geometry

4.2 Development of liquid phase fraction and velocity

The ParaView outlook of phase fraction (α) and U (velocity) for case 3 is visualized in this part. First, the development of velocity is displayed at certain time steps: 0, 0.5, 1, 7.5, 8.5, 10 (s). Then the evolution of α at time steps: 0, 0.5, 1, 4.5, 10(s) are observed.

As it can be seen from Figure 4-4 to Figure 4-9, at time zero the fields given the velocity value in 0 folder (as initial condition) are visible at inlets of the liquid. By running the simulation, we can see the liquid flowing downward with raise in velocity and then it slows down behind the porous zone due to the resistance of the structure and the velocity drops. Liquid flows slowly through the packing and at time step 7.5 it exists the porous media entering no resistance region of the bottom of the column.

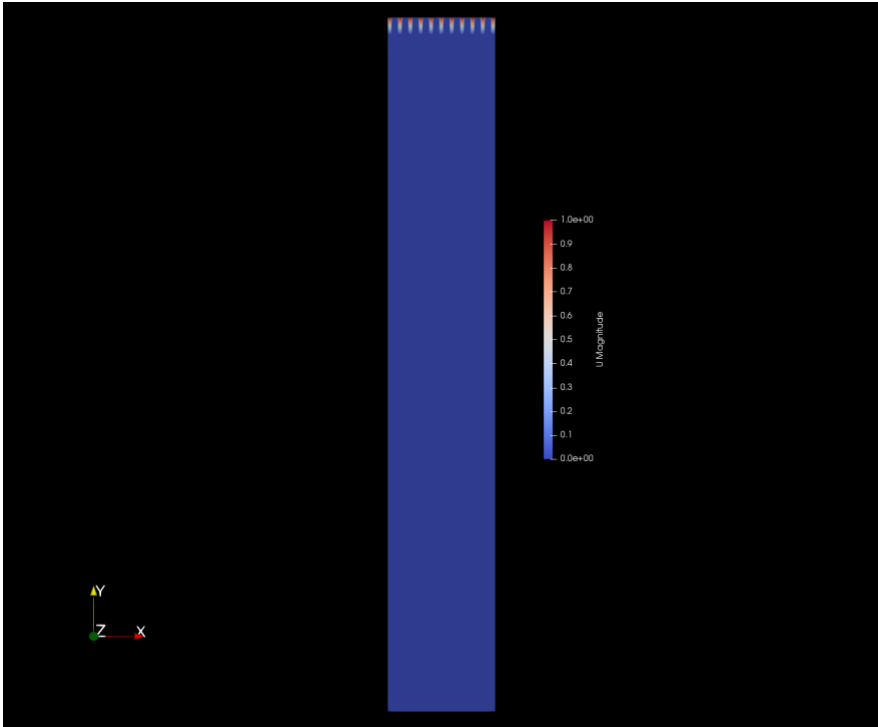


Figure 4-4 Velocity field for case 3 at time 0 (s)

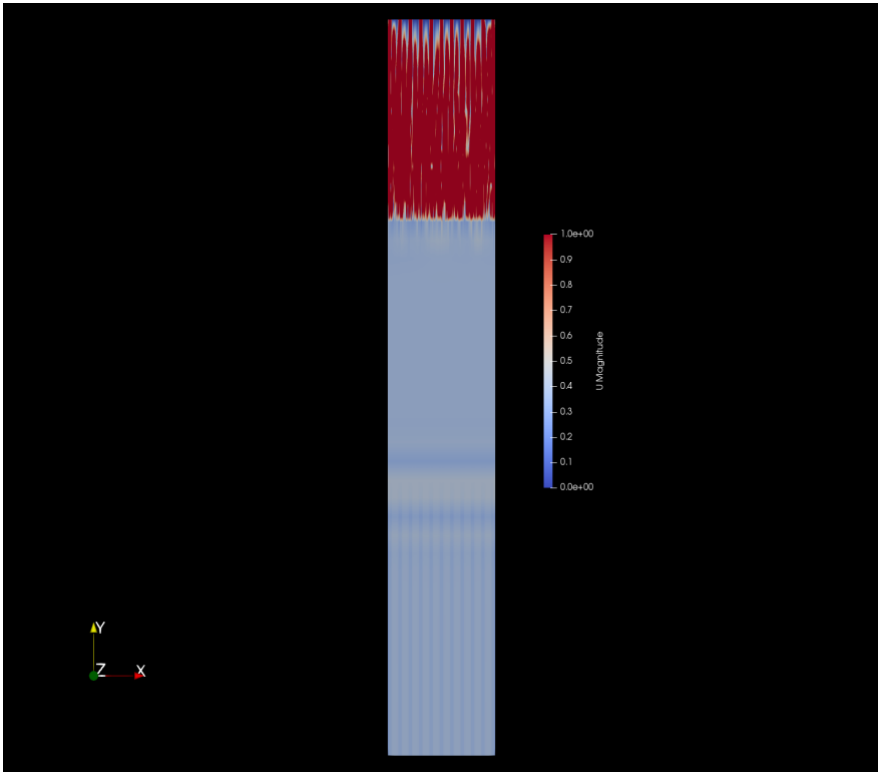


Figure 4-5 Velocity field for case 3 at time 0.5 (s)

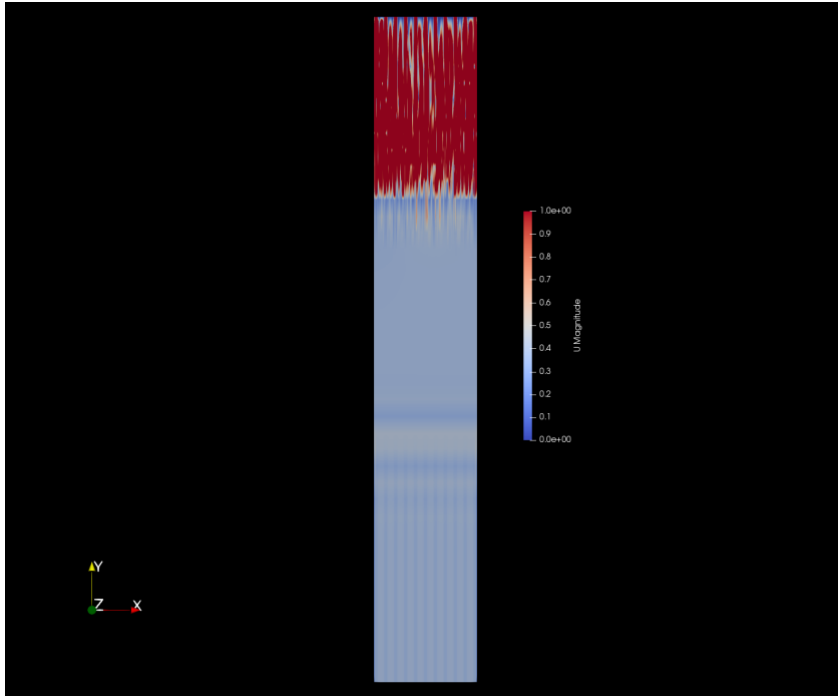


Figure 4-6 Velocity field for case 3 at time 1 (s)

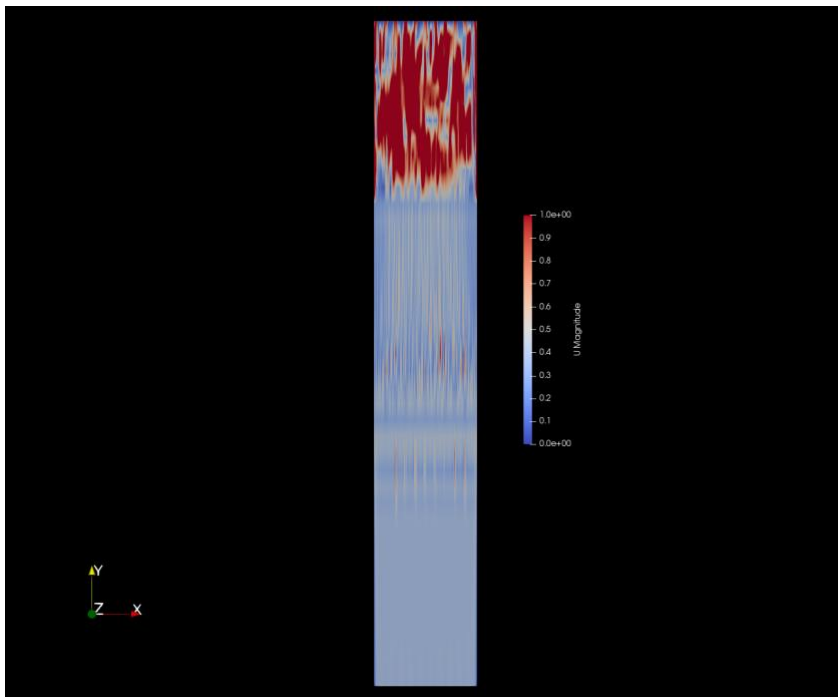


Figure 4-7 Velocity field for case 3 at time 7.5 (s)

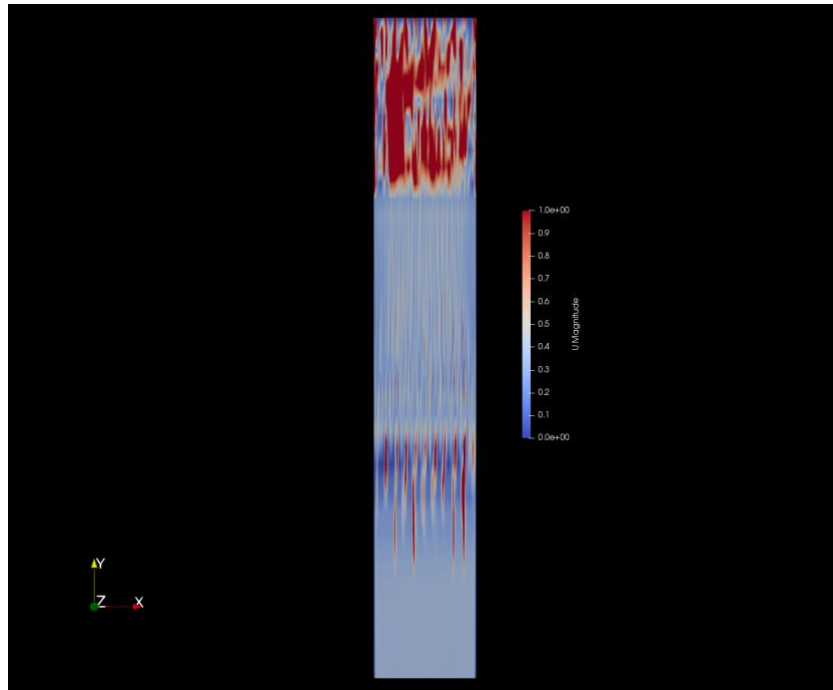


Figure 4-8 Velocity field for case 3 at time 8.5 (s)

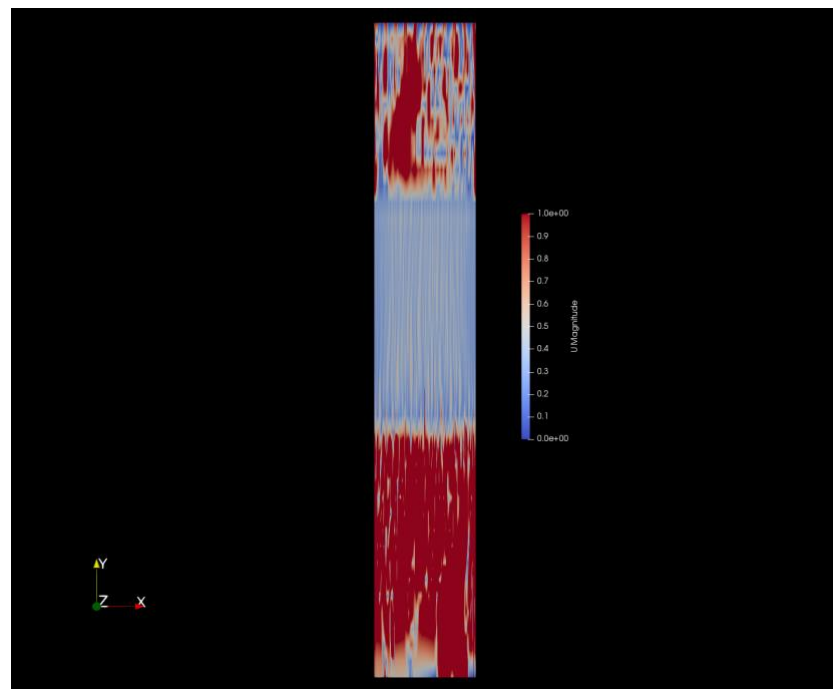


Figure 4-9 Velocity field for case 3 at time 10 (s)

In this tutorial case, the system is filled with air at time 0 and the liquid starts flowing in the system after time 0. From Figure 4-10 to Figure 4-14 we can see the liquid phase fraction in the stripper entering the geometry from above and slowly flowing through the packing.

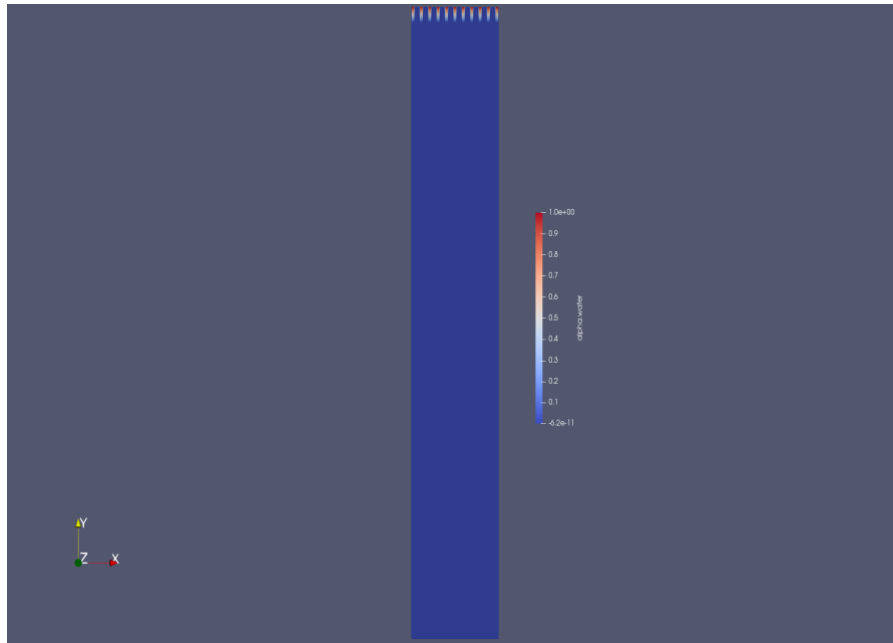


Figure 4-10 Liquid phase fraction at time 0 (s)

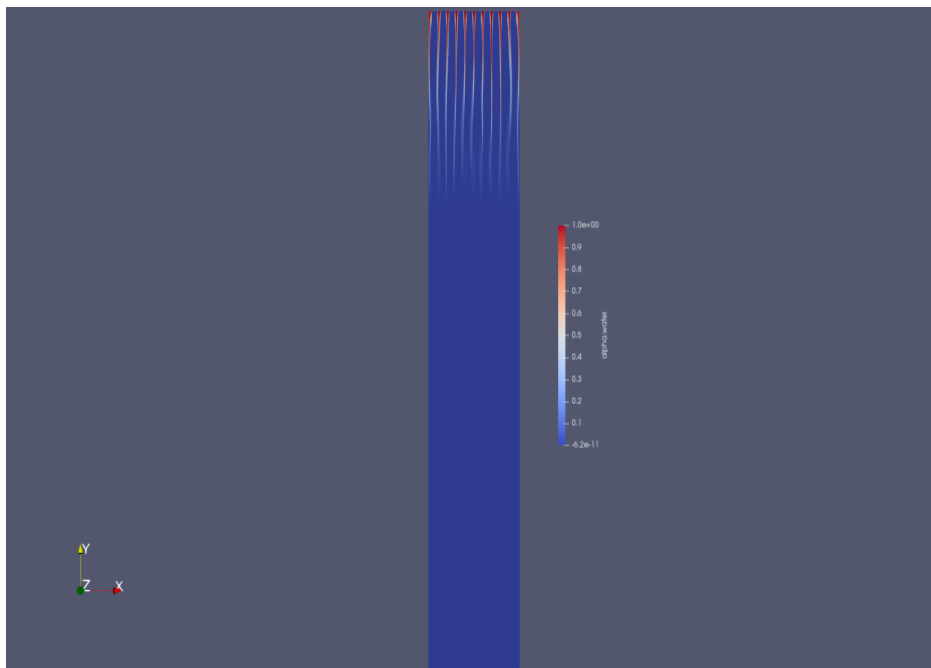


Figure 4-11 Liquid phase fraction at time 0.5 (s)

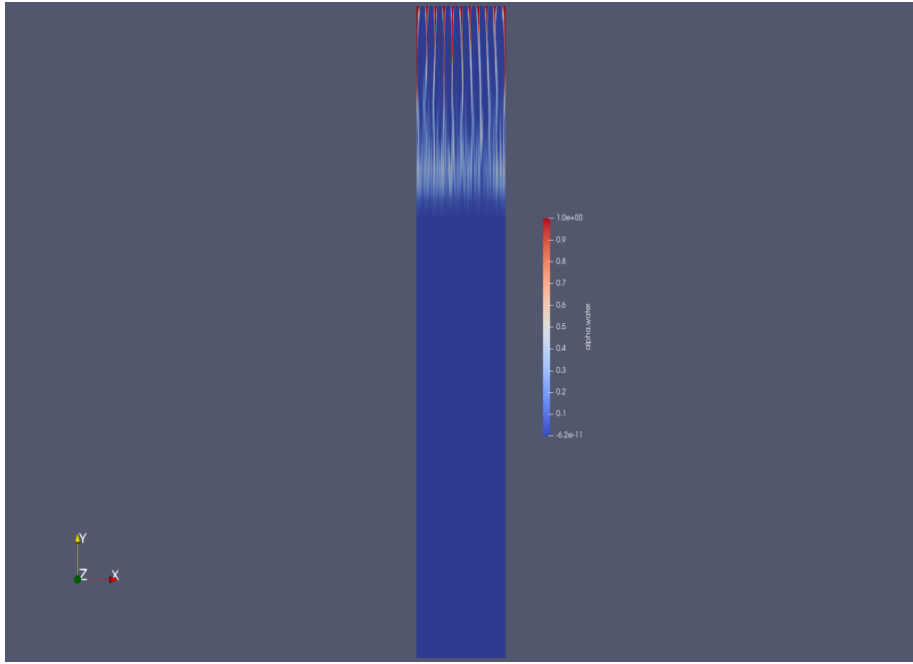


Figure 4-12 Liquid phase fraction at time 1(s)

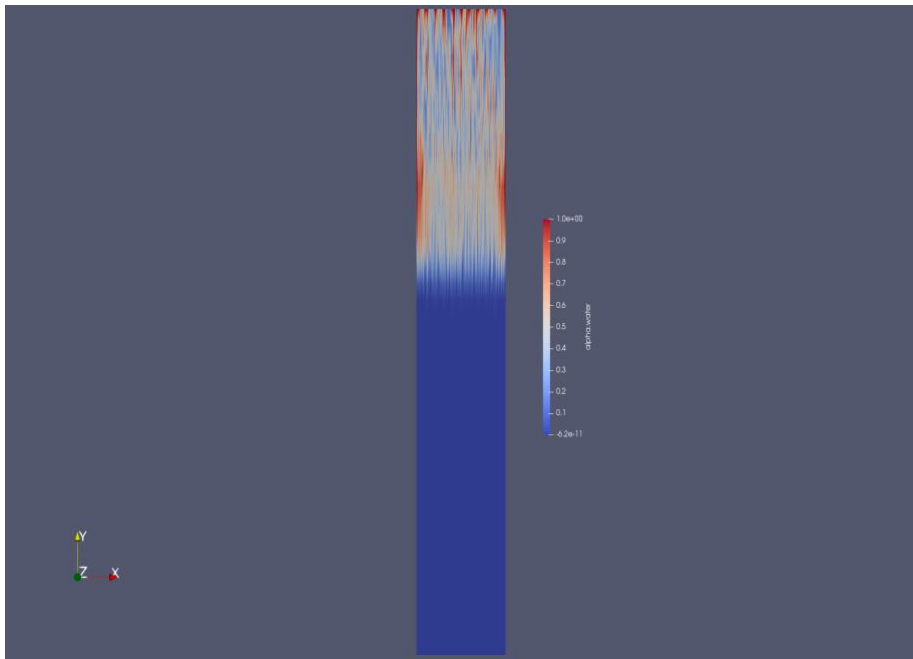


Figure 4-13 Liquid phase fraction at time 4.5 (s)

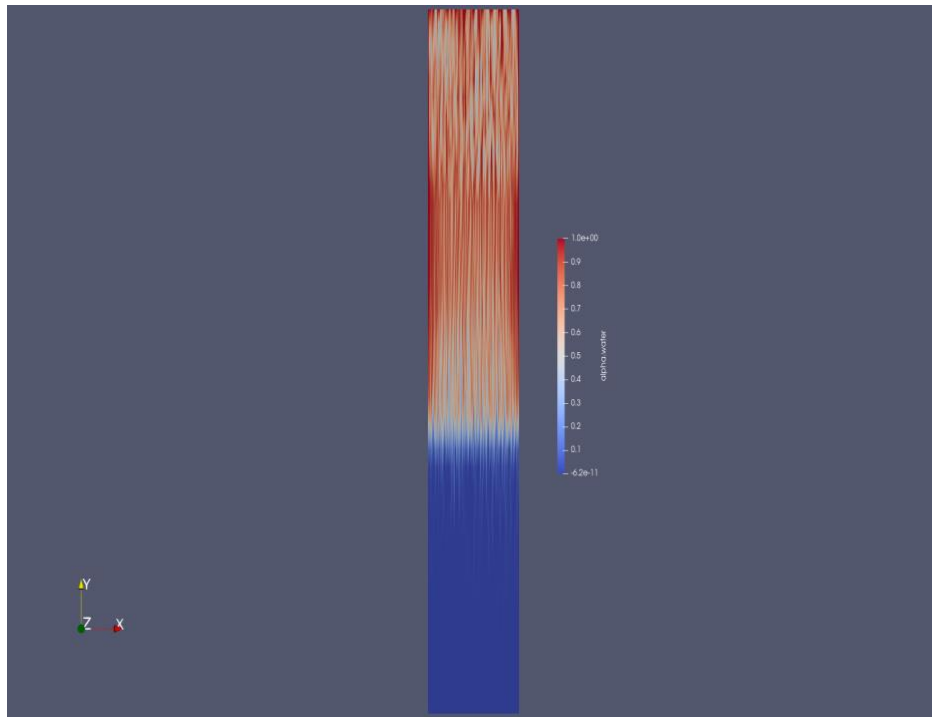


Figure 4-14 Liquid phase fraction at time 10 (s)

4.3 Simulation comparison for case 2 to 4

What is variable from case 1 to 4 is the Darcy coefficient (d or D) from Darcy-Forchheimer equation (2.19). Figure 4-15 to Figure 4-17 compare the simulation for these cases at similar time steps. Case 1 has not been reported since it gives close enough results to the second case.

Comparing Figure 4-15, Figure 4-16 and Figure 4-17 we can see that the higher the D value the less the permeability of the porous zone which results in improving vortex flow (recirculation) above and below the porous zone.

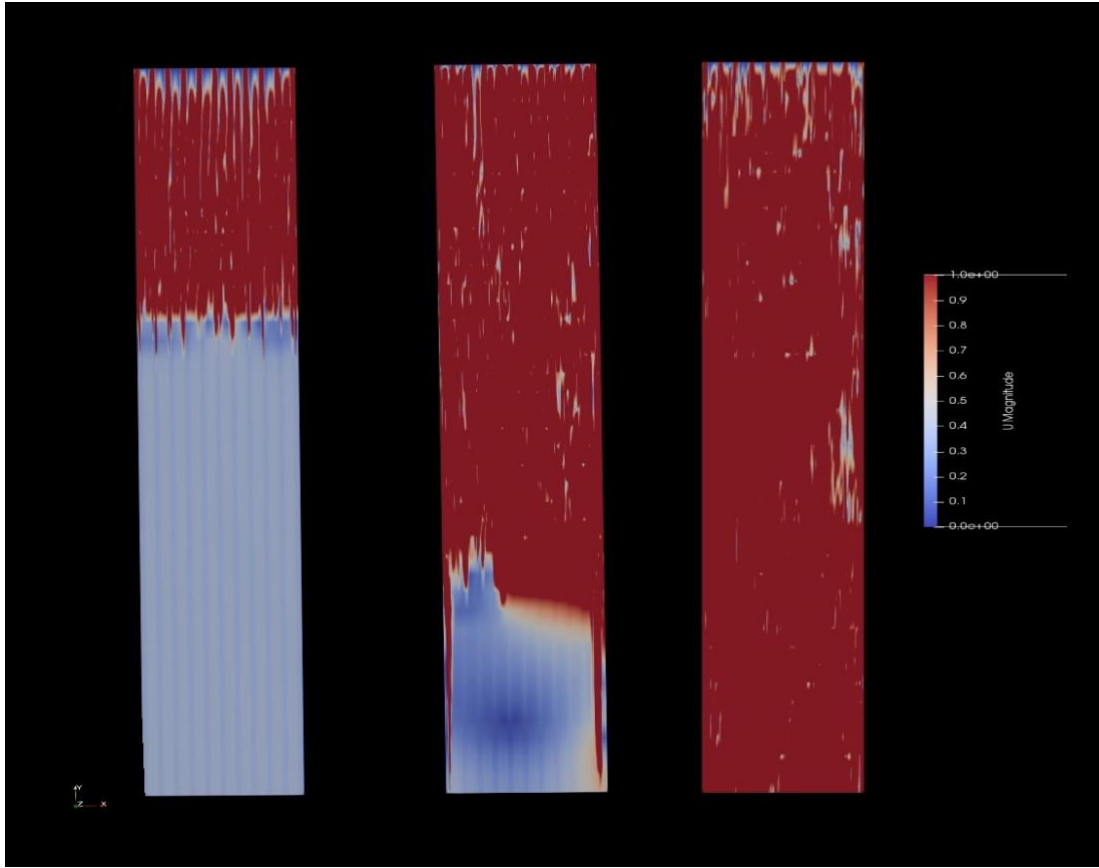


Figure 4-15 velocity profile of case 2 at time steps 0.5, 1 and 7.5 from left to right

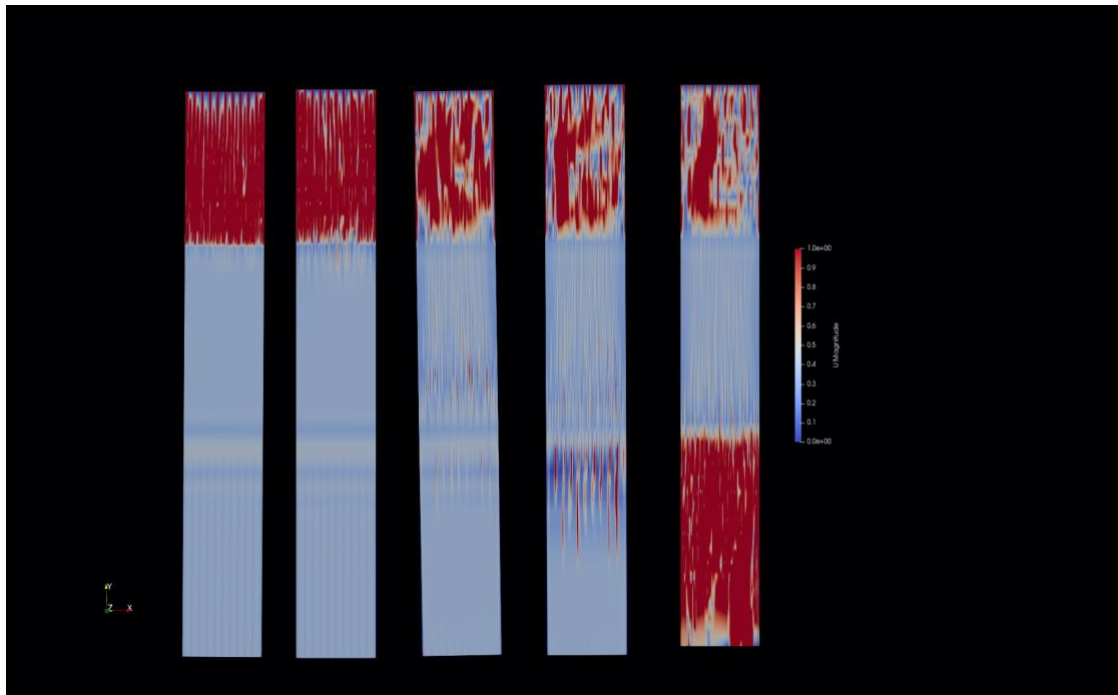


Figure 4-16 Velocity profile of case 3 at time steps 0.5, 1, 7.5, 8.5, 10 from left to right

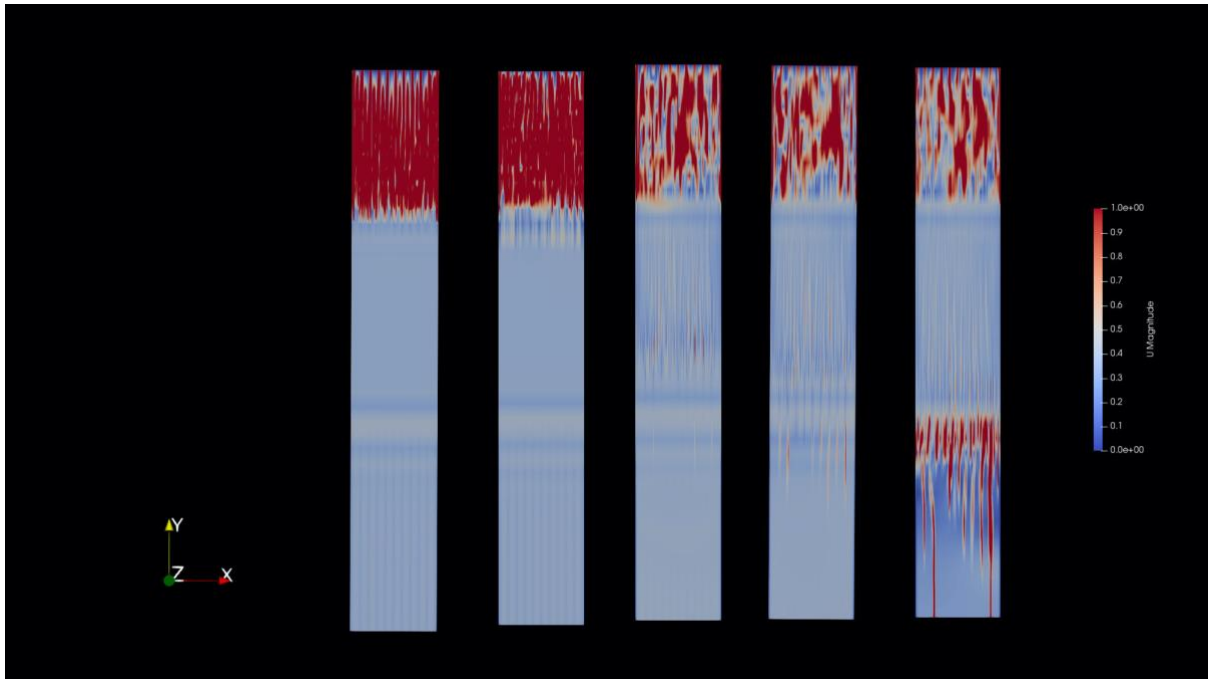


Figure 4-17 Velocity profile of case 4 at time steps 0.5, 1, 7.5, 8.5, 10 from left to right

Observation of flow development by changing the velocity in Figure 4-16 for velocity 1 m/s, Figure 4-18 and Figure 4-19 shows that for a system with velocity below 1 and high D value the liquid cannot easily flow through the porous zone. This can cause loading or recirculation in the system above the packing area.

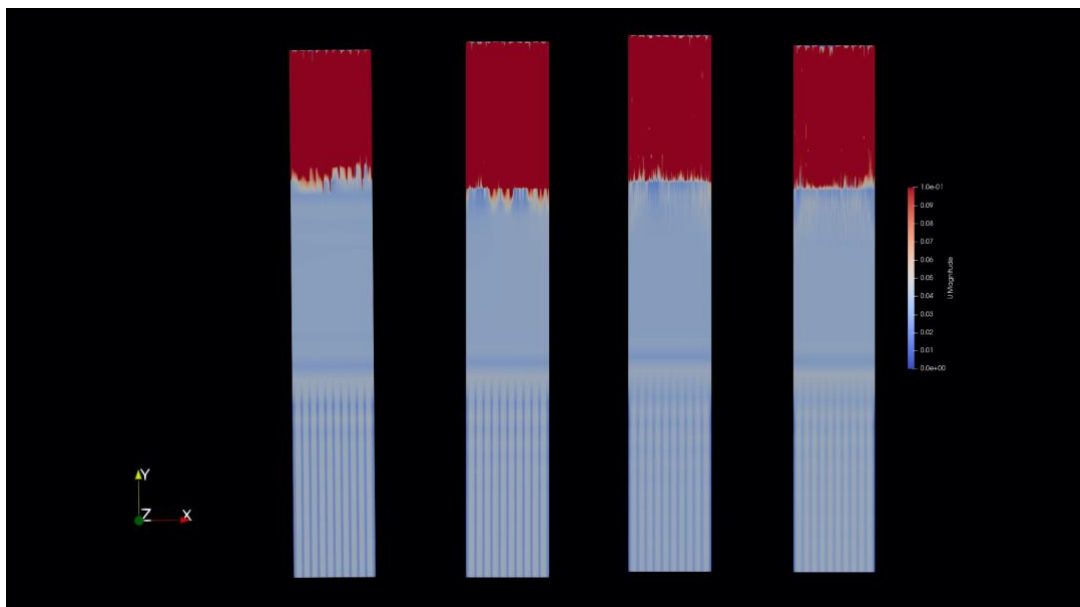


Figure 4-18 Velocity profile of case 5 ($U=0.1$ m/s) at time steps 0.5, 1, 7.5, 10

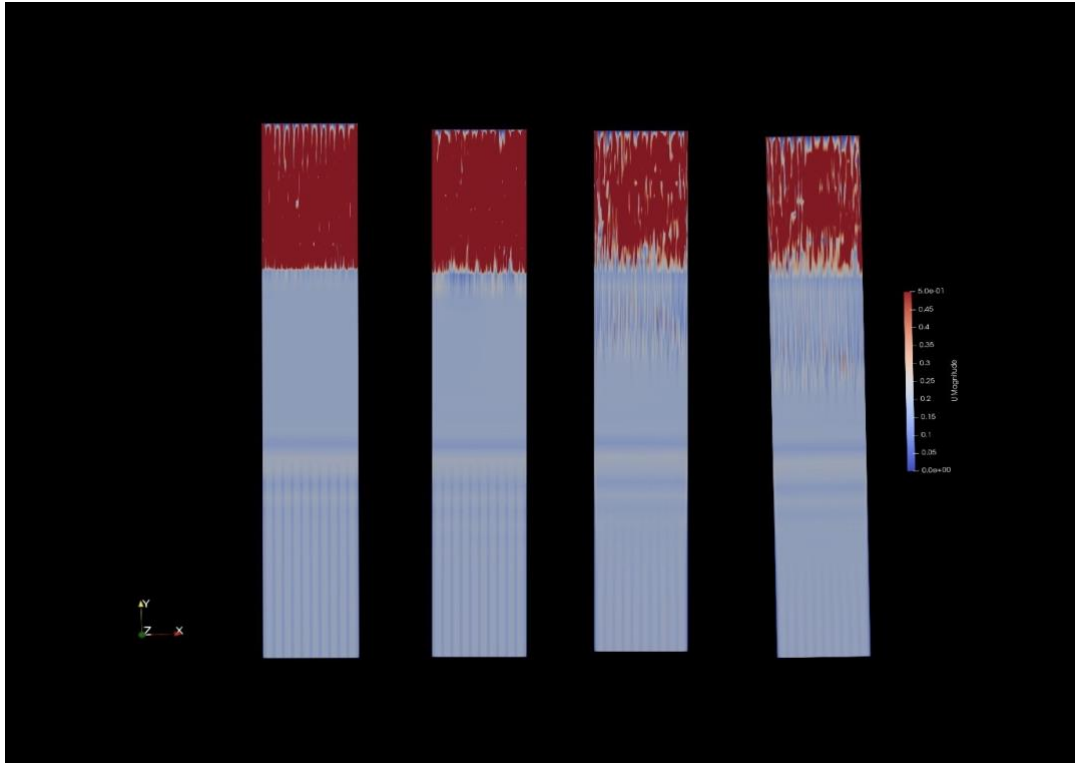


Figure 4-19 Velocity profile of case 6 ($U=0.5$ m/s) at time steps 0.5, 1, 7.5, 10

4.4 Delta P over porosity

The pressure drop profile of all seven cases at time step = 6(s) are shown below.

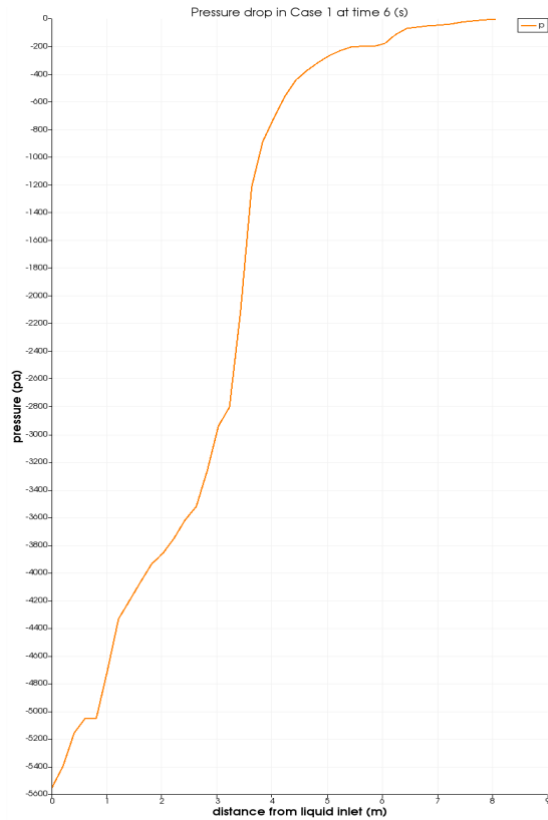


Figure 4-20 Pressure difference in case 1 over y-axis.

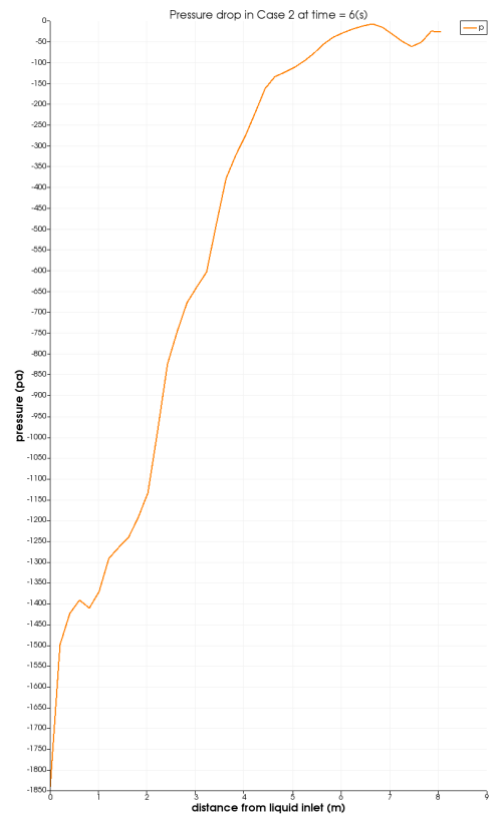


Figure 4-21 Pressure difference in case 2 over y-axis

As expected, for cases with lower Darcy values (Figure 4-20 and Figure 4-21) where permeability is high pressure is increasing along y-axis due to the packing residence. What is uncertain here is the negative sign of the pressure.

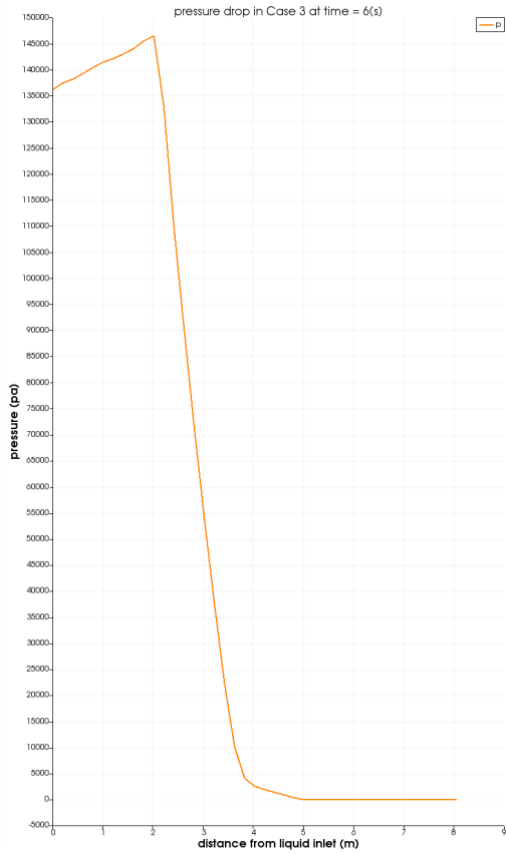


Figure 4-22 Pressure difference in case 3 over y-axis.

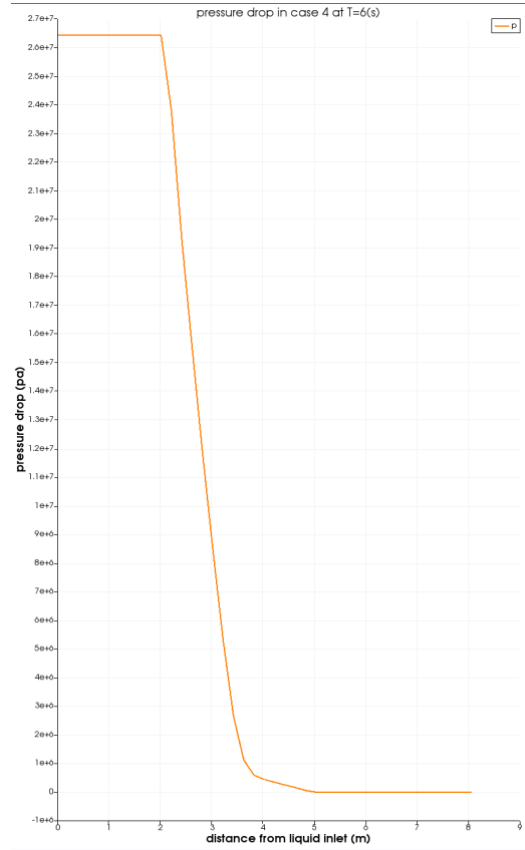


Figure 4-23 Pressure difference in case 4 over y-axis.

The pressure for cases with higher D value (Figure 4-22 and Figure 4-23) is decreasing along the column. This is an expected behavior since the liquid hardly flows through the porous zone and this causes a pressure drop in this region. The behavior on case 7 (same D value with higher velocity) is similar to case 3.

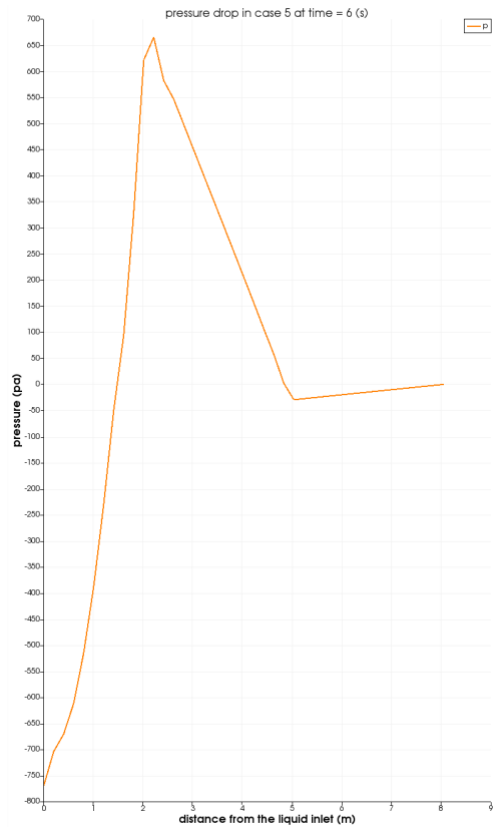


Figure 4-24 Pressure difference in case 5 over y-axis.

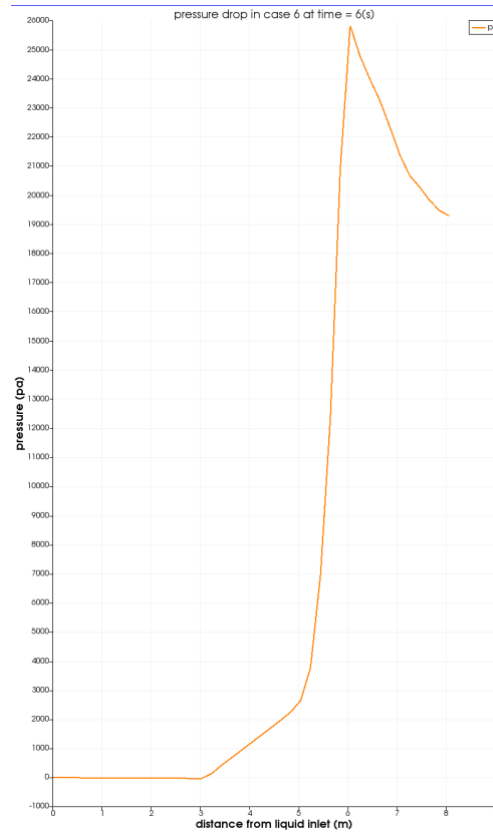


Figure 4-25 Pressure difference in case 6 over y-axis.

From Figure 4-18 and Figure 4-19 for case 5 & 6 we know that when the liquid flows in the system with small velocities and it does not penetrate in the packing section easily. This will cause a dramatic increase of pressure above the packed section since the liquid is flowing continuously into the system and yet cannot flow downwards. The effect of gas pressure is dominating and does not let the liquid to flow in the system. This is mainly the case for when the velocity is 0.1 [m/s]. The flow gets easier when the velocity increases to 0.5 m/s.

4.5 Velocity in the packing

In last part we observed that in case 1 & 2 the pressure increases in the system, in case 3, 4 & 7 it decreases and in case 5 & 6 it raises dramatically before the packing and then it decreases when it flows out of the packed region. From this pattern we can predict the behavior of velocity for each case keeping this in mind that for the first case and second case there are uncertainties in pressure values which will definitely result in unstable velocity evolution.

In this part the velocity plots of different cases are illustrated at time step 6.

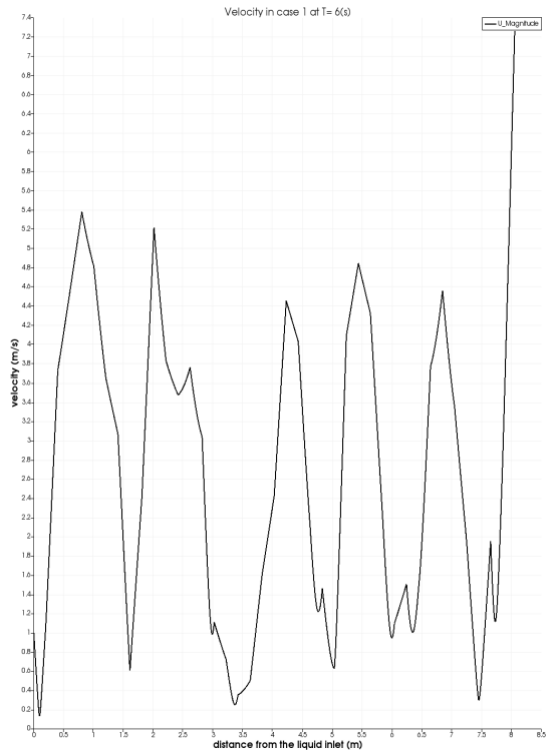


Figure 4-26 Velocity distribution of case 1 along y-axis at time = 6 (s)

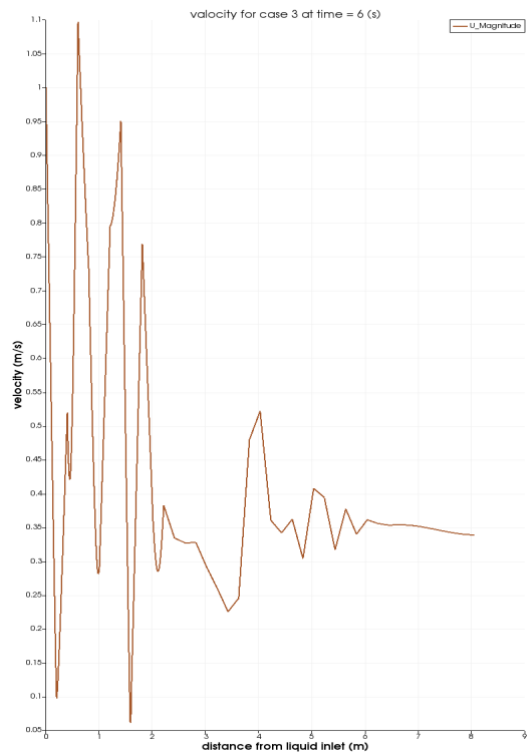


Figure 4-27 Velocity distribution of case 3 along y-axis at time = 6 (s)

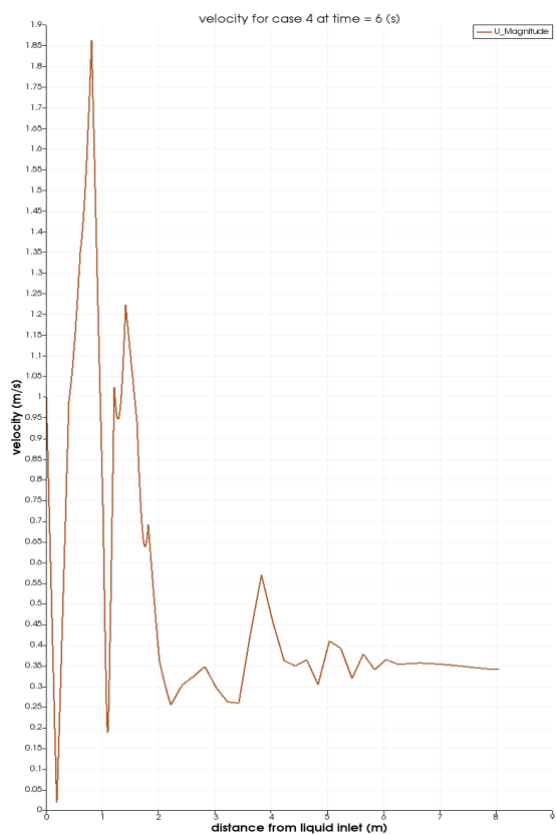


Figure 4-28 Velocity distribution of case 4 along y-axis at time = 6 (s)

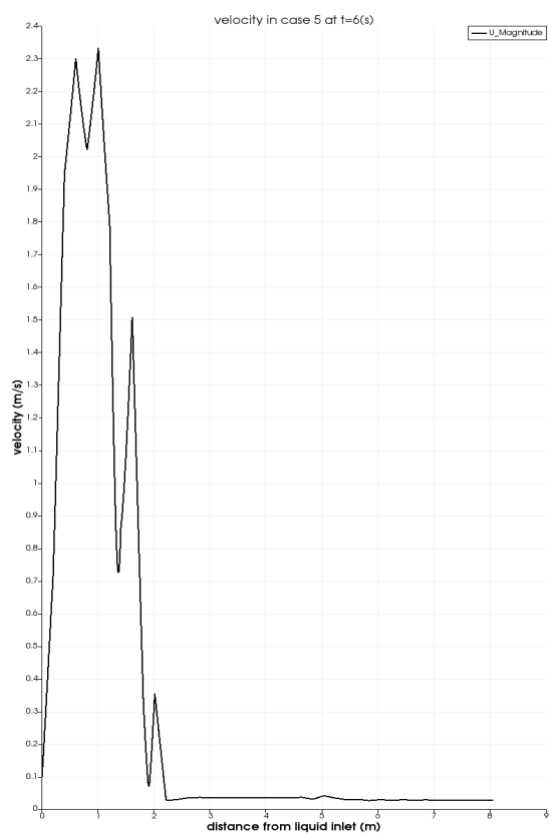


Figure 4-29 Velocity distribution of case 5 along y-axis at time = 6 (s)

The velocity profile of case 1 and 2 are similar hence, I just report one of them in here which is shown in Figure 4-26. As expected before, there is fluctuation in velocity field in case 1. In case 3 we can see that the liquid flow velocity decreases after entering the porous zone due to higher Darcy value and it does not change very much along the packing section. The velocity ranges between 0.2 to 0.55 [m/s] inside the porous media. The same behavior is observed for case 4 in Figure 4-28 as well.

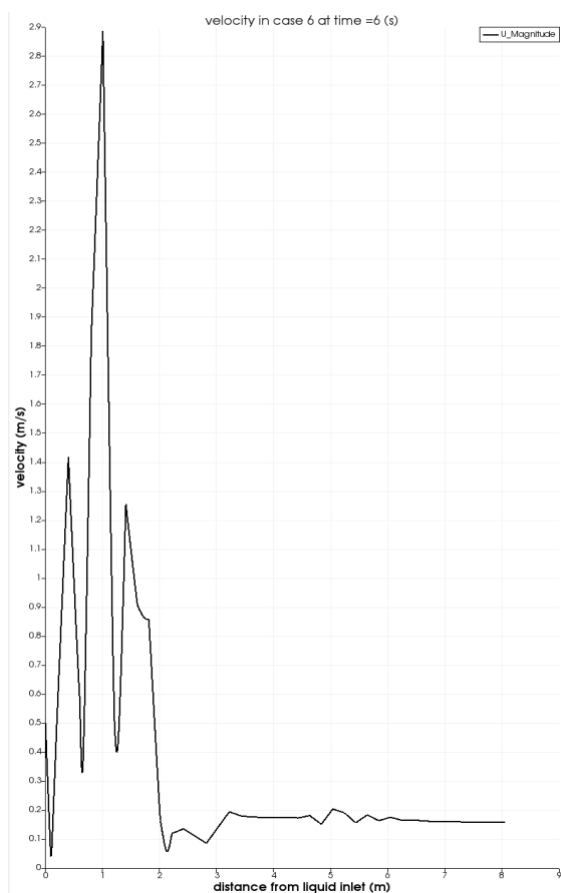


Figure 4-30 Velocity distribution of case 6 along y-axis at time = 6 (s)

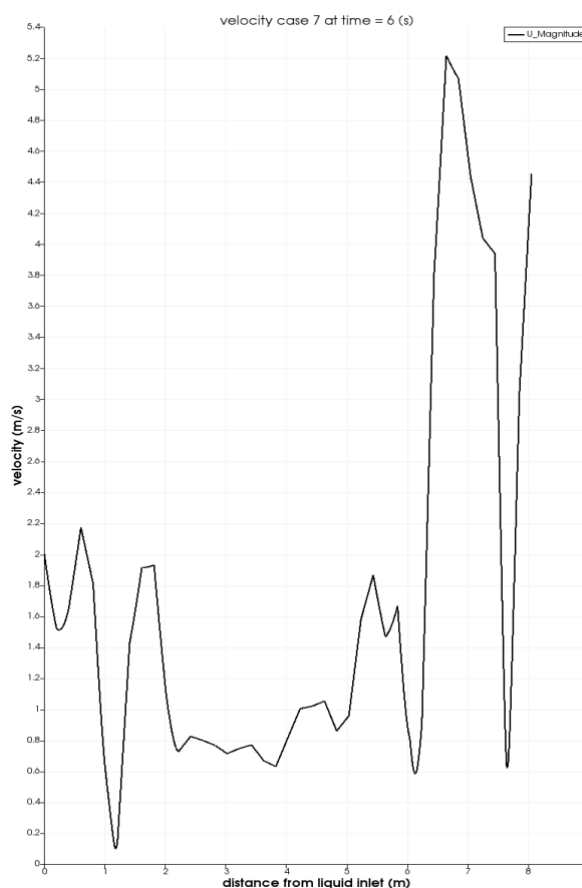


Figure 4-31 Velocity distribution of case 7 along y-axis at time = 6 (s)

In cases 5 & 6 (Figure 4-29 and Figure 4-30) where the velocity is smaller than case 3, we know that the liquid holds up in the upper packing section and cannot easily cross the porous zone. This will cause noticeable increase in velocity above packing area and dramatic decrease from the start of the packing section. Another thing that should be noted is that this velocity profiles are showing the velocity magnitude. What we expect in this chaotic region is the possibility of recirculation of flow and this is unwanted in this system. In the last case (Figure 4-31) the velocity increases after exiting the porous zone due to gravitational force and no prevention in geometry.

5 Discussion

In chapter 4 the result of this work is written with explanations on what is observed in each case by changing different variables in the system. It was noticed that some cases behave as it is expected but in some other cases there are some uncertainties regarding the results. In this chapter I would like to discuss what are the uncertainties and what could be the probable cause of these unexpected or unwanted outcome, as well as suggestions of possible changes that might help with error reduction.

5.1 Discussion of uncertainties

At first, I would like to discuss the behavior of fluid in upper part of the packing in the simulations. The simulation Glyph view (showing the vector field) shows a strange behavior for some cases in this region. The flow in the system is natural for case 1 and 2 but then with increase of Darcy value and velocity we can observe that the fluid recirculation starts to intensify. This flux in the system will cause the velocity vector in y direction to switch sign in the system which is completely unwanted because we are interested for liquid to flow into the porous section so that the mass transfer between the two phases can take place. In my opinion, this simulation case is so sensitive to velocity range and the optimum velocity should be something more that 0.1 and less than 1 [m/s].

Another unreasonable observation is the negative pressure signs in the first and second case but this phenomenon is possible when running an incompressible fluid and setting the operating pressure to zero (or any low pressure). In incompressible case the pressure is gauge pressure and not absolute pressure. Gauge pressure is the pressure relative to the ambient atmospheric pressure. So, the negative pressure in here is a consequence of boundary condition. It is said by David Hargreaves that: *“This is because the pressure gradient enters the Navier-Stokes equations and so it is pressure differences that drive the flow. So, in regions of separated flow, the low pressure inside that region will be relative to the lowest fixed pressure in your system and may well go negative.”* [31]

5.2 Evaluation of alternative simulations

Alternative simulation cases for this system can be the use of true geometrical construction as it is in TCM. This study only considers the stripper column from below the inter-bed liquid distributor. What can be done is to create the geometry for multi-beds with inter-bed liquid distribution. It is observed in one of the literatures that the simulation case has more valid results when it is carried out with the actual physical state [9].

In order to prevent the unexpected results discussed above different possibilities in boundary conditions can be executed. This can consist of both geometrical boundaries and operational boundary conditions. In addition, exact operation condition was unavailable for this case but

working outside the operating condition can be another cause to the behavior of this set up. And as mentioned above, since the case is velocity sensitive the more in detail study of whether laminar or turbulent simulation should be executed for each velocity is of an importance.

5.3 Discussion for further works

This case was established to simulate and solve an operational problem at TCM Mongstad but due to the lack of base case for the CFD stripper column it was mainly dedicated to establish a CFD simulation of the desorber. So, my suggestions for further improvement of this task and solving the problem are as below:

- Trying reactingMultiphaseEulerFoam solver which can model phase change, mass transfer and chemical reactions
- Simulation of the turbulent scenario for the multiphase simulations
- More in detail study of the effect of different factors such as velocity range or Darcy value and simulations of more cases with variant values

6 Conclusion

Liquid distribution on packing section of a desorption column was simulated and visualized by OpenFOAM and ParaView. The effect of Darcy coefficient (coefficient of permeability) and liquid inlet velocity on the flow distribution was demonstrated.

Observations shows that by increasing the Darcy coefficient of the porous zone the permeability of liquid in this region decreases. Systems with lower Darcy coefficient values act like a plain column and the systems with higher Darcy value face a chaotic fluid flow above the packing due to the resistance of the structure.

The study of liquid velocity variation shows that very low velocities (e.g. 0.1 [m/s]) cannot flow in the system easily due to the pressure dominance. To my understanding in these cases the force of the pressure is dominating and it is the reason for resistance of liquid inflow. Increase in velocity leads the system to a more desirable results but there is a limit for velocity in the system and I believe higher velocities (e.g. 1 [m/s]) have to be simulated with a turbulence case. The velocity fields of almost all cases show that the alteration of velocity decreases after entering the porous zone.

References

- [1] Mai Bui, Nina E. Fløc, Thomas de Cazenovec and Niall Mac Dowella, "Demonstrating flexible operation of the Technology Centre Mongstad (TCM) CO₂ capture plant," *International Journal of Greenhouse Gas Control*, vol. 93, no. 102879, 2020.
- [2] P. C. Chen and Yan-Lin Lai, "Optimization in the Stripping Process of CO₂ Gas Using Mixed Amines," *MDPI*, 2019.
- [3] V. P. Z. H.-O. P. D. R. J. S. P. S. A. P. W. M.-O. C. P. R. P. S. C. J. M. Y. C. X. Z. M. G. E. L. T. M. M. T. a. T. W. (. Masson-Delmotte, " Summary for Policymakers. In: Global Warming of 1.5°C. An IPCC Special Report on the impacts of global warming of 1.5°C above pre-industrial levels and related global greenhouse gas emission pathways, in the context of strengthening the global response t," IPCC, 2018.
- [4] A. Stangeland, "Bellona," 9 October 2009. [Online]. Available: [Link](#). [Accessed May 2021].
- [5] IEA, "IEA (2021)," Global Energy Review 2021, Paris, 2021.
- [6] Paweł Niegodajew and Dariusz Asendrych, "Amine based CO₂ capture – CFD simulation of absorber performance," *Applied Mathematical Modelling*, vol. 40, p. 10222–10237, 2016.
- [7] M. Isoz, "CFD Study of Gas Flow Through Structured Separation Columns Packings Mellapak 250.X and Mellapak 250.Y," in *Topical Problems of Fluid Mechanics 2017*, Prague, 2017.
- [8] Paweł Niegodajew, Dariusz Asendrych and Stanisław Drobniak, "Numerical modeling of the CO₂desorption process coupled with phasetransformation and heat transfer in a CCS installation," *Journal of Power Technologies*, vol. 93, no. 5, pp. 354-362, 2013.
- [9] Dela Quarne Gbadagoa, Hyun-Taek Ohb, Dong-Hoon Ohb, Chang-Ha Leeb and Min Oha, "CFD simulation of a packed bed industrial absorber with interbed liquid distributors," *International Journal of Greenhouse Gas Control*, 2020.
- [10] Li Yang, Fang Liu, Kozo Saito and Kunlei Liu, "CFD Modeling on Hydrodynamic Characteristics of Multiphase Counter-Current Flow in a Structured Packed Bed for Post-Combustion CO₂ Capture," *MDPI energies*, 2018.
- [11] Y. Haroun, L. Raynal and D. Legendre, "Mass transfer and liquid hold-up determination in structured packing by CFD," *Chemical Engineering Science*, vol. 75, pp. 342-348, 2012.
- [12] Dan Yu, Dapeng Cao, Zhazhan Li and Qunsheng Li, "Experimental and CFD studies on the effects of surface texture on liquid thickness, wetted area and mass transfer in wave-like structured packings," *Chemical Engineering Research and Design*, vol. 129, pp. 170-181, 2018.

- [13] Dung A. Pham, Young-II Lim, Hyunwoo Jee, Euisub Ahn and Yongwon Jung, "Porous media Eulerian computational fluid dynamics (CFD) model of amine absorber with structured-packing for CO₂ removal," *Chemical Engineering Science*, pp. 259-270, 2015.
- [14] Ludovic Raynal, Christophe Boyer and Jean-Pierre Ballaguet, "Liquid Holdup and Pressure Drop Determination in Structured Packing with CFD Simulations," *The Canadian Journal of Chemical Engineering*, pp. 871-879, 2008.
- [15] H. K. Versteeg and W. Malalasekera, *An introduction to computational fluid dynamics the finite volume method*, Pearson Education Limited, 2007.
- [16] NASA, "National aeronautics and space administration," 05 May 2015. [Online]. Available: <https://www.grc.nasa.gov/www/k-12/airplane/nseqs.html>. [Accessed 3 May 2021].
- [17] C. Greenshields, "CFD Direct," 10 July 2018. [Online]. Available: <https://cfd.direct/openfoam/user-guide/v6-fvschemes/>. [Accessed 2021].
- [18] C. Greenshields, "Cfd Direct," 21 July 2020. [Online]. Available: <https://cfd.direct/openfoam/user-guide/v8-fvSchemes/#x20-1450004.5>. [Accessed 2021].
- [19] A. Wimshurst, "[CFD] Porous Zones in CFD," 10 September 2019. [Online]. Available: <https://www.youtube.com/watch?v=sOQMXxoKFQM>. [Accessed 2021].
- [20] N. Dukhan and Carel A. Minjeur II, "A two-permeability approach for assessing flow properties in metal foam," *Journal of Porous Materials*, vol. 18, no. August 2011, pp. 417-424, 2011.
- [21] D. A. Tillman, D. N. Duong and N. S. Harding, *Solid Fuel Blending: principles, practices, and problems*, Butterworth-Heinemann, 2012.
- [22] "Openfoam," openCFD Ltd, 2019. [Online]. Available: <https://www.openfoam.com/>. [Accessed 2021].
- [23] J. Lorenzo, "github," 20 June 2018. [Online]. Available: <https://github.com/joslogom/tankFoamCase>. [Accessed 2021].
- [24] C. Greenshields, "Solution and algorithm control," CFD Direct, July 2020. [Online]. Available: <https://cfd.direct/openfoam/user-guide/v8-fvSolution/#x21-1590004.6.3>. [Accessed 2021].
- [25] S. S. Karunaratne, Dag A. Eimer and Lars E. Øi, "Physical Properties of MEA + Water + CO₂ Mixtures in Postcombustion CO₂ Capture: A Review of Correlations and Experimental Studies," *Hindawi*, vol. 2020, no. 05 March, 2020.
- [26] F. Yang, Xiaopo Wang, Wei Wang and Zhigang Liu, "Densities and Excess Properties of Primary Amines in Alcoholic Solutions," *Chemical engineering and data*, vol. 58, no. 18 February, pp. 785 - 791, 2013.
- [27] [Online]. Available: <https://www.afs.enea.it/project/neptunius/docs/fluent/html/ug/node233.htm>.
- [28] H. E. Hafsteinsson, "Porous Media in OpenFOAM," Chalmers, 2009.

- [29] P. Havaej, "Hyper Lyceum," October 2020. [Online]. Available: <https://www.youtube.com/watch?v=jy43aZcXNXA>.
- [30] C. Greenshields, "CFD Direct," OpenFOAM Foundation, 10 July 2018. [Online]. Available: <https://cfd.direct/openfoam/user-guide/v6-case-file-structure/>. [Accessed 21 April 2021].
- [31] "ResearchGate," 27 May 2016. [Online]. Available: <https://www.researchgate.net/post/In-fluent-Why-is-there-negative-static-pressure-while-I-set-the-operating-pressure-0-Pa>.
- [32] C. Greenshields, "OpenFOAM v8 User Guide: 7.1 Thermophysical models," 21 July 2021. [Online]. Available: <https://cfd.direct/openfoam/user-guide/v8-thermophysical/>. [Accessed 2021].
- [33] I. Woodard & Curran, "Treatment of Air Discharges from Industry," in *Industrial Waste Treatment Handbook*, 2006.
- [34] A. Wimshurst, "[CFD] The k - epsilon Turbulence Model," 15 June 2019. [Online]. Available: <https://www.youtube.com/watch?v=fOB91zQ7HJU&t=1282s>. [Accessed 2021].
- [35] Rajesh K.Singh, Zhijie Xu and Chao Wang, "Residence time distribution in a structured packing unit for monitoring aerosol emissions," *International Journal of Greenhouse Gas Control*, vol. 79, no. December, pp. 181-192, 2018.
- [36] Y. Haroun, L.Raynal and D.Legendre, "Mass transfer and liquid hold-up determination in structured packing by CFD," *Chemical Engineering Science*, vol. 75, no. 20 march, pp. 342-348, 2012.
- [37] Alexander Olenberg, Wadim Reschetnik, Gunter Kullmer and Eugeny Y. Kenig, "Optimization of structured packings using twisted tape inserts," *Chemical Engineering Research and Design*, vol. 132, pp. 1-8, 2018.
- [38] A. Wimshurst, "Fluid Mechanics 101," 24 02 2021. [Online]. Available: <https://www.youtube.com/watch?v=SVYXNICeNWA&t=353s>. [Accessed 2021].
- [39] P. Havaej, "Hyper Lyceum," October 2020. [Online]. Available: <https://www.hyperlyceum.com/product/flow-through-a-porous-media-using-openfoam/>.

Appendices

Appendix A <blockMeshDict>

```
1 |/*-----*- C++ -*-----*/
2 | =====
3 | \\\ / F i e l d | OpenFOAM: The Open Source CFD Toolbox
4 | \\\ / O p e r a t i o n | Version: 5
5 | \\\ / A n d | Web: www.OpenFOAM.org
6 | \\\ / M a n i p u l a t i o n |
7 |*-----*/
8 FoamFile
9 {
10 version 2.0;
11 format ascii;
12 class dictionary;
13 object blockMeshDict;
14 }
15 // ***** //
16
17 convertToMeters 1;
18
19 vertices
20 (
21 (0 0 0)
22 (0.005 0 0)
23 (.045 0 0)
24 (0.125 0 0)
25 (0.165 0 0)
26 (0.245 0 0)
27 (0.285 0 0)
28 (0.365 0 0)
29 (0.405 0 0)
30 (0.485 0 0)
31 (0.525 0 0)
32 (0.605 0 0)
33 (0.645 0 0)
34 (0.725 0 0)
35 (0.765 0 0)
36 (0.845 0 0)
37 (0.885 0 0)
38 (0.965 0 0)
39 (1.005 0 0)
40 (1.085 0 0)
41 (1.125 0 0)
42 (1.205 0 0)
43 (1.245 0 0)
44 (1.250 0 0)
45
46 (1.250 8.050 0)
47 (1.245 8.050 0)
48 (1.205 8.050 0)
49 (1.125 8.050 0)
50 (1.085 8.050 0)
51 (1.005 8.050 0)
52 (0.965 8.050 0)
53 (0.885 8.050 0)
54 (0.845 8.050 0)
55 (0.765 8.050 0)
56 (0.725 8.050 0)
57 (0.645 8.050 0)
58 (0.605 8.050 0)
59 (0.525 8.050 0)
```


59 (0.525 8.050 0)
60 (0.485 8.050 0)
61 (0.405 8.050 0)
62 (0.365 8.050 0)
63 (0.285 8.050 0)
64 (0.245 8.050 0)
65 (0.165 8.050 0)
66 (0.125 8.050 0)
67 (0.045 8.050 0)
68 (0.005 8.050 0)
69 (0 8.050 0)
70
71 (0 0 0.1)
72 (0.005 0 0.1)
73 (.045 0 0.1)
74 (0.125 0 0.1)
75 (0.165 0 0.1)
76 (0.245 0 0.1)
77 (0.285 0 0.1)
78 (0.365 0 0.1)
79 (0.405 0 0.1)
80 (0.485 0 0.1)
81 (0.525 0 0.1)
82 (0.605 0 0.1)
83 (0.645 0 0.1)
84 (0.725 0 0.1)
85 (0.765 0 0.1)
86 (0.845 0 0.1)
87 (0.885 0 0.1)
88 (0.965 0 0.1)
89 (1.005 0 0.1)
90 (1.085 0 0.1)
91 (1.125 0 0.1)
92 (1.205 0 0.1)
93 (1.245 0 0.1)
94 (1.250 0 0.1)
95
96 (1.250 8.050 0.1)
97 (1.245 8.050 0.1)
98 (1.205 8.050 0.1)
99 (1.125 8.050 0.1)
100 (1.085 8.050 0.1)
101 (1.005 8.050 0.1)
102 (0.965 8.050 0.1)
103 (0.885 8.050 0.1)
104 (0.845 8.050 0.1)
105 (0.765 8.050 0.1)
106 (0.725 8.050 0.1)
107 (0.645 8.050 0.1)
108 (0.605 8.050 0.1)
109 (0.525 8.050 0.1)
110 (0.485 8.050 0.1)
111 (0.405 8.050 0.1)
112 (0.365 8.050 0.1)
113 (0.285 8.050 0.1)
114 (0.245 8.050 0.1)
115 (0.165 8.050 0.1)
116 (0.125 8.050 0.1)

```

117         (0.045 8.050 0.1)
118         (0.005 8.050 0.1)
119         (0 8.050 0.1)
120
121
122 );
123
124 blocks
125 (
126
127     hex (0 1 46 47 48 49 94 95) (5 40 1) simpleGrading (1 1 1)
128     hex (1 2 45 46 49 50 93 94) (40 40 1) simpleGrading (1 1 1)
129     hex (2 3 44 45 50 51 92 93) (10 40 1) simpleGrading (1 1 1)
130     hex (3 4 43 44 51 52 91 92) (40 40 1) simpleGrading (1 1 1)
131     hex (4 5 42 43 52 53 90 91) (10 40 1) simpleGrading (1 1 1)
132     hex (5 6 41 42 53 54 89 90) (40 40 1) simpleGrading (1 1 1)
133     hex (6 7 40 41 54 55 88 89) (10 40 1) simpleGrading (1 1 1)
134     hex (7 8 39 40 55 56 87 88) (40 40 1) simpleGrading (1 1 1)
135     hex (8 9 38 39 56 57 86 87) (10 40 1) simpleGrading (1 1 1)
136     hex (9 10 37 38 57 58 85 86) (40 40 1) simpleGrading (1 1 1)
137     hex (10 11 36 37 58 59 84 85) (10 40 1) simpleGrading (1 1 1)
138     hex (11 12 35 36 59 60 83 84) (40 40 1) simpleGrading (1 1 1)
139     hex (12 13 34 35 60 61 82 83) (10 40 1) simpleGrading (1 1 1)
140     hex (13 14 33 34 61 62 81 82) (40 40 1) simpleGrading (1 1 1)
141     hex (14 15 32 33 62 63 80 81) (10 40 1) simpleGrading (1 1 1)
142     hex (15 16 31 32 63 64 79 80) (40 40 1) simpleGrading (1 1 1)
143     hex (16 17 30 31 64 65 78 79) (10 40 1) simpleGrading (1 1 1)
144     hex (17 18 29 30 65 66 77 78) (40 40 1) simpleGrading (1 1 1)
145     hex (18 19 28 29 66 67 76 77) (10 40 1) simpleGrading (1 1 1)
146     hex (19 20 27 28 67 68 75 76) (40 40 1) simpleGrading (1 1 1)
147     hex (20 21 26 27 68 69 74 75) (10 40 1) simpleGrading (1 1 1)
148     hex (21 22 25 26 69 70 73 74) (40 40 1) simpleGrading (1 1 1)
149     hex (22 23 24 25 70 71 72 73) (5 40 1) simpleGrading (1 1 1)
150
151
152 );
153
154 edges
155 (
156 );
157
158 boundary
159 (
160
161
162     inlet
163     {
164         type patch;
165         faces
166         (
167             (45 93 94 46)
168             (43 91 92 44)
169             (41 89 90 42)
170             (39 87 88 40)
171             (37 85 86 38)
172             (35 83 84 36)
173             (33 81 82 34)
174             (31 79 80 32)
175             (29 77 78 30)

```

```

175         (29 77 78 30)
176         (27 75 76 28)
177         (25 73 74 26)
178
179     );
180 }
181 }
182
183 outlet
184 {
185     type patch;
186     faces
187     (
188         (1 49 48 0)
189         (2 50 49 1)
190         (3 51 50 2)
191         (4 52 51 3)
192         (5 53 52 4)
193         (6 54 53 5)
194         (7 55 54 6)
195         (8 56 55 7)
196         (9 57 56 8)
197         (10 58 57 9)
198         (11 59 58 10)
199         (12 60 59 11)
200         (13 61 60 12)
201         (14 62 61 13)
202         (15 63 62 14)
203         (16 64 63 15)
204         (17 65 64 16)
205         (18 66 65 17)
206         (19 67 66 18)
207         (20 68 67 19)
208         (21 69 68 20)
209         (22 70 69 21)
210         (23 71 70 22)
211     )
212 );
213 }
214 }
215
216 leftWall
217 {
218     type symmetryPlane;
219     faces
220     (
221         (47 95 48 0)
222     )
223 );
224 }
225
226 rightWall
227 {
228     type symmetryPlane;
229     faces
230     (
231         (24 72 71 23)
232     )
233 );
234 }
235
236 top
237 {
238     type patch;
239     faces
240     (
241         (46 94 95 47)
242         (44 92 93 45)
243         (42 90 91 43)
244         (40 88 89 41)
245         (38 86 87 39)
246         (36 84 85 37)

```

```
246         (36 84 85 37)
247         (34 82 83 35)
248         (32 80 81 33)
249         (30 78 79 31)
250         (28 76 77 29)
251         (26 74 75 27)
252         (24 72 73 25)
253
254     );
255 }
256
257
258 );
259
260 mergePatchPairs
261 (
262 );
263
264 // ***** //
```

Appendix B <topoSetDict>

```
1 |/*-----*- C++ -*-----*/
2 |
3 | ===== |
4 | \ \ \ \ \ \ | F i e l d | OpenFOAM: The Open Source CFD Toolbox
5 | \ \ \ \ \ \ | O p e r a t i o n | Version: 4.0
6 | \ \ \ \ \ \ | A n d | Web: www.OpenFOAM.org
7 | \ \ \ \ \ \ | M a n i p u l a t i o n |
8 |-----*/
9 FoamFile
10 {
11     version      2.0;
12     format       ascii;
13     class        dictionary;
14     object       topoSetDict;
15 }
16 // ***** //
17
18
19     actions
20 (
21     {
22         name      porousCellSet;
23         type      cellSet;
24         action    new;
25         source    boxToCell;
26         sourceInfo
27         {
28             box (0 3 0)(1.250 6 0.1);
29         }
30     }
31     {
32         name      porousCells;
33         type      cellZoneSet;
34         action    new;
35         source    setToCellZone;
36         sourceInfo
37         {
38             set porousCellSet;
39         }
40     }
41 );
42
43 // ***** //
```

Appendix C <controlDict>

```
1 /*-----*- C++ -*-----*/
2 |=====|
3 | \ \ \ \ \ | F i e l d | OpenFOAM: The Open Source CFD Toolbox
4 | \ \ \ \ \ | O p e r a t i o n | Version: 5
5 | \ \ \ \ \ | A n d | Web: www.OpenFOAM.org
6 | \ \ \ \ \ | M a n i p u l a t i o n |
7 /*-----*/
8 FoamFile
9 {
10     version      2.0;
11     format        ascii;
12     class         dictionary;
13     location      "system";
14     object        controlDict;
15 }
16 // ***** //
17
18 application      interFoam;
19
20 startFrom        latestTime;
21
22 startTime        0;
23
24 stopAt           endTime;
25
26 endTime          10;
27
28 deltaT           0.1;
29
30 writeControl     adjustableRunTime;
31
32 writeInterval    0.5;
33
34 purgeWrite       0;
35
36 writeFormat      ascii;
37
38 writePrecision   6;
39
40 writeCompression uncompressed;
41
42 timeFormat       general;
43
44 timePrecision    6;
45
46 runTimeModifiable yes;
47
48 adjustTimeStep   yes;
49
50 maxCo            1;
51 maxAlphaCo       1;
52
53 maxDeltaT        1;
54
55
56 // ***** //
```

Appendix D <fvSchemes>

```
1 |/*-----* C++ -*-----*/
2 | =====
3 | \ \ / F i e l d | OpenFOAM: The Open Source CFD Toolbox
4 | \ \ / O p e r a t i o n | Version: 5
5 | \ \ / A n d | Web: www.OpenFOAM.org
6 | \ \ / M a n i p u l a t i o n |
7 |*-----*/
8 FoamFile
9 {
10   version      2.0;
11   format       ascii;
12   class        dictionary;
13   location     "system";
14   object       fvSchemes;
15 }
16 // *****
17
18 ddtSchemes
19 {
20   default      Euler;
21 }
22
23 gradSchemes
24 {
25   default      Gauss linear;
26 }
27
28 divSchemes
29 {
30   div(rhoPhi,U) Gauss linearUpwind grad(U);
31   div(phi,alpha) Gauss vanLeer;
32   div(phiRb,alpha) Gauss linear;
33   div(((rho*nuEff)*dev2(T(grad(U)))) Gauss linear;
34 }
35
36 laplacianSchemes
37 {
38   default      Gauss linear corrected;
39 }
40
41 interpolationSchemes
42 {
43   default      linear;
44 }
45
46 snGradSchemes
47 {
48   default      corrected;
49 }
50
51
52 // ***** //
```

Appendix E <fvSolution>

```

1 /*-----* C++ *-----*/
2 |=====|
3 | \ / \ / | F i e l d | OpenFOAM: The Open Source CFD Toolbox
4 | \ / \ / | O p e r a t i o n | Version: 5
5 | \ / \ / | A n d | Web: www.OpenFOAM.org
6 | \ / \ / | M a n i p u l a t i o n |
7 |-----*-----*/
8 FoamFile
9 {
10     version      2.0;
11     format        ascii;
12     class         dictionary;
13     location      "system";
14     object        fvSolution;
15 }
16 // *****
17
18 solvers
19 {
20     "alpha.water.*" // This is for alpha.MEA but it has not been renamed
21     {
22         nAlphaCorr      2;
23         nAlphaSubCycles 1;
24         cAlpha          1;
25
26         MULESCorr      yes;
27         nLimiterIter   5;
28
29         solver          smoothSolver;
30         smoother        symGaussSeidel;
31         tolerance       1e-8;
32         relTol          0;
33     }
34
35     "pcorr.*"
36     {
37         solver          PCG;
38         preconditioner  DIC;
39         tolerance       1e-5;
40         relTol          0;
41     }
42
43     p_rgh
44     {
45         solver          PCG;
46         preconditioner  DIC;
47         tolerance       1e-07;
48         relTol          0.05;
49     }
50
51     p_rghFinal
52     {
53         $p_rgh;
54         relTol          0;
55     }
56
57     U
58     {
59         solver          smoothSolver;
60         smoother        symGaussSeidel;
61         tolerance       1e-06;
62         relTol          0;
63     }
64 }
65
66 PIMPLE
67 {
68     momentumPredictor  no;
69     nOuterCorrectors   1;
70     nCorrectors        3;
71     nNonOrthogonalCorrectors 0;
72     pRefCell  0; //added
73     pRefValue 0; //added
74 }
75
76 relaxationFactors
77 {
78     equations
79     {
80         "*" 1;
81     }
82 }
83
84

```


Appendix F <transportProperties>

```
1 /*-----* C++ *-----*\
2 | ===== |
3 | \\ / Field | OpenFOAM: The Open Source CFD Toolbox |
4 | \\ / Operation | Version: 5 |
5 | \\ / A nd | Web: www.OpenFOAM.org |
6 | \\ / Manipulation | |
7 /*-----*\
8 FoamFile
9 {
10   version      2.0;
11   format       ascii;
12   class        dictionary;
13   location     "constant";
14   object       transportProperties;
15 }
16 // ***** //
17
18 phases (water air); //The water and air are not renamed here but the values are respective
19                // (MEA CO2)
20 water //MEA
21 {
22   transportModel  Newtonian;
23   nu              1e-06;
24   rho             1006;
25 }
26
27 air //CO2
28 {
29   transportModel  Newtonian;
30   nu              8.36e-06;
31   rho             2;
32 }
33
34 sigma           0.072;
35
36 // ***** //
```

Appendix G <fvOptions>

```

1 /*-----*- C++ -*-----*/
2 |=====|
3 | \ \ / / F i e l d | OpenFOAM: The Open Source CFD Toolbox
4 | \ \ / / O p e r a t i o n | Version: 4.0
5 | \ \ / / A n d | Web: www.OpenFOAM.org
6 | \ \ / / M a n i p u l a t i o n |
7 /*-----*- C++ -*-----*/
8 FoamFile
9 {
10     version      2.0;
11     format       ascii;
12     class        dictionary;
13     location     "constant";
14     object       fvOptions;
15 }
16 // ***** //
17
18 porosity1
19 {
20     type          explicitPorositySource;
21     active        yes;
22
23     explicitPorositySourceCoeffs
24     {
25         selectionMode    cellZone;
26         cellZone         porousCells;
27
28         type             DarcyForchheimer;
29
30         // D 100;
31         // D 200;
32         D 500e6;
33         // D 8.85e10;
34
35
36         DarcyForchheimerCoeffs
37         {
38             d ($D $D $D);
39             f (0 0 0);
40
41             coordinateSystem
42             {
43                 type    cartesian;
44                 origin (0 0 0);
45                 coordinateRotation
46                 {
47                     type    axesRotation;
48                     e1 (1 0 0);
49                     e2 (0 1 0);
50                 }
51             }
52         }
53     }
54 }
55
56
57 // ***** //

```

Appendix H <alpha>

```
1 |/*-----* C++ *-----*/
2 |=====|
3 | \ \ / F i e l d | OpenFOAM: The Open Source CFD Toolbox
4 | \ \ / O p e r a t i o n | Website: https://openfoam.org
5 | \ \ / A n d | Version: 8
6 | \ \ / M a n i p u l a t i o n |
7 |*-----*/
8 FoamFile
9 {
10     version      2.0;
11     format        ascii;
12     class         volScalarField;
13     location      "0";
14     object        alpha.liquid;
15 }
16 // ***** //
17
18 dimensions      [0 0 0 0 0 0];
19
20 internalField    uniform 0;
21
22 boundaryField
23 {
24     inlet
25     {
26         type          inletOutlet;
27         inletValue    uniform 1;
28         value         uniform 1;
29     }
30     outlet
31     {
32         type          zeroGradient;
33     }
34     leftWall
35     {
36         type          zeroGradient;
37     }
38     rightWall
39     {
40         type          zeroGradient;
41     }
42     top
43     {
44         type          zeroGradient;
45     }
46     defaultFaces
47     {
48         type          empty;
49     }
50 }
51 }
52
53
54 // ***** //
```

Appendix I <p_rgh>

```
1 |/*-----* C++ *-----*/
2 | |=====|
3 | | \ \ / / F i e l d | OpenFOAM: The Open Source CFD Toolbox
4 | | \ \ / / O p e r a t i o n | Version: 5
5 | | \ \ / / A n d | Web: www.OpenFOAM.org
6 | | \ \ / / M a n i p u l a t i o n |
7 |/*-----*
8 FoamFile
9 {
10     version      2.0;
11     format        ascii;
12     class         volScalarField;
13     object        p_rgh;
14 }
15 // ***** //
16
17 dimensions      [1 -1 -2 0 0 0];
18
19 internalField   uniform 0;
20
21 boundaryField
22 {
23     leftWall
24     {
25         type      zeroGradient;
26     }
27
28     rightWall
29     {
30         type      zeroGradient;
31     }
32
33     top
34     {
35         type      zeroGradient;
36     }
37
38     inlet
39     {
40         type      fixedFluxPressure;
41         value     uniform 0;
42     }
43
44     outlet
45     {
46         type      totalPressure;
47         p0        uniform 0;
48     }
49
50     defaultFaces
51     {
52         type      empty;
53     }
54 }
55
56 // ***** //
```

Appendix J <U>

```
1 |/*-----* C++ *-----*/
2 | ===== |
3 | \ \ \ \ \ \ | F i e l d | OpenFOAM: The Open Source CFD Toolbox
4 | \ \ \ \ \ \ | O p e r a t i o n | Version: 5
5 | \ \ \ \ \ \ | A n d | Web: www.OpenFOAM.org
6 | \ \ \ \ \ \ | M a n i p u l a t i o n |
7 |/*-----*
8 FoamFile
9 {
10     version      2.0;
11     format       ascii;
12     class        volVectorField;
13     location     "0";
14     object       U;
15 }
16 // ***** //
17
18 dimensions      [0 1 -1 0 0 0];
19
20 internalField   uniform (0 0 0);
21
22 boundaryField
23 {
24     leftWall
25     {
26         type      noSlip;
27     }
28     rightWall
29     {
30         type      noSlip;
31     }
32
33     top
34     {
35         type      noSlip;
36     }
37
38     inlet
39     {
40         type      fixedValue;
41         value     uniform (0 -1 0);
42     }
43     outlet
44     {
45         type      pressureInletOutletVelocity;
46         value     uniform (0 0 0);
47     }
48     defaultFaces
49     {
50         type      empty;
51     }
52 }
53
54
55 // ***** //
```